Lehrstuhl für
Technische Dynamik
Prof. Dr.-Ing. habil. Sigrid Leyendecker

Report
Institute of Applied Dynamics
2022

Friedrich-Alexander-Universität
Technische Fakultät

Prof. Dr.-Ing. habil. S. Leyendecker
Lehrstuhl für Technische Dynamik
Friedrich-Alexander-Universität Erlangen-Nürnberg
Immerwahrstrasse 1
91058 Erlangen
Tel.: 09131 8561000
Fax.: 09131 8561011
www: https://www.ltd.tf.fau.de

Editors: E. Fleischmann, D. Phansalkar

Contents

1 Preface

This report gives a summary of the scientific and teaching activities of the Institute of Applied Dynamics (LTD) at the Friedrich-Alexander-Universität Erlangen-Nürnberg during the year 2022. The members of LTD are passionately working on topics such as multibody dynamics and robotics, motion capturing, biomechanics, structure preserving methods and optimal control.
Many thanks to our technical, scientific and admin staff at LTD and also to all the students involved to make it a successful year at the Institute of Applied Dynamics. We wish you an enjoyable time glancing through our annual report.

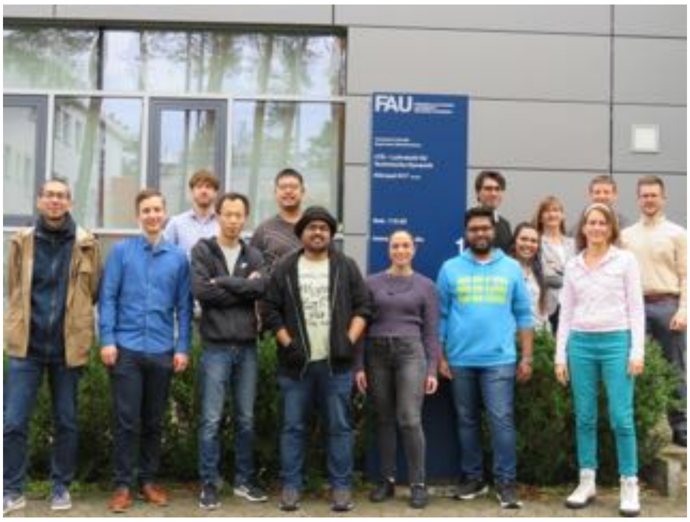

2 Team

head of institute
Prof. Dr.-Ing. habil. Sigrid Leyendecker

team assistant

Beate Hegen	
Hanna Mahmud-Munir	from 01.11.2022

technical staff
M.Sc. Elisa Fleischmann
M.Sc. Markus Lohmayer

akademischer Rat
Dr.-Ing. Giuseppe Capobianco, Akad. Rat

postdoc
Dr. Rodrigo Sato Martín de Almagro
Dr.-Ing. Dengpeng Huang

scientific staff

M.Sc.hons. Xiyu Chen	
M.Sc. Birte Coppers	
M.Sc. Simon Heinrich	
M.Sc. David Holz	
M.Sc. Deepak Balasaheb Jadhav	from 01.05.2022
M.Sc. Denisa Martonová	
M.Sc. Dhananjay Phansalkar	
M.Sc. Eduard Sebastian Scheiterer	
M.Sc. Matthias Schubert	until 30.11.2022
M.Sc. Martina Stavole	
M.Sc. Theresa Wenger	until 31.03.2022

students

Murat Aydinli	Johanna Bloehs	Yijing Cao
Xiaojing Chen	Claude Jöel Motsebo Fotso	Lieselotte Daub
Mohamad Dekelbab	Lou Ebert	Jakob Fischer
Lisa Fischer	Johanna Fredrich	Marc Gadinger
Nahrain Gtari	Roman Hohenbichler	Julian Hübner
Yuan Jin	Zandantsetseg Khishigdulam	Lea Köstler
Sonja Kuhn	Julian Lang	Markus Menzel
Zakaryapour Mohammadhosein	Manuel Ott	Felix Pfister
Arne Pietsch	Julian Pollet	Abdul Qudoos
Nivashini Radhakrishnan	Jenni Reitinger	Marietta Stegmaier
Fajar Falah Supono	Michelle Tautenhahn	Yi Zhu

Student assistants are mainly active as tutors for young students in basic and advanced lectures at the Bachelor and Master level. Their contribution to high quality teaching is indispensable, thus financial support from various funding sources is gratefully acknowledged.


G. Capobianco


X. Chen


B. Coppers


E. Fleischmann


B. Hegen


S. Heinrich


D. Holz


D. Huang


D. Jadhav


M. Lohmayer

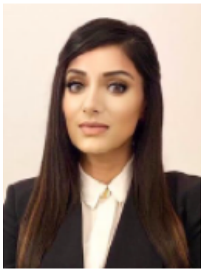
H. Mahmud-Munir


D. Martonová


D. Phansalkar


R.T. Sato


E.S. Scheiterer


M. Schubert


M. Stavole


T. Wenger


S. Leyendecker

3 Research

3.1 ETN – THREAD

The Institute of Applied Dynamics takes part in the ETN (European Training Network) project "Joint Training on Numerical Modelling of Highly Flexible Structures for Industrial Applications – THREAD" funded by the European Commission's Marie Skłodowska Curie Programme which is part of Horizon 2020. The project is coordinated by Prof. Dr. Martin Arnold from the Institute of Mathematics at the Martin Luther University Halle-Wittenberg (MLU). Prof. Dr.-Ing. habil. Sigrid Leyendecker is principal investigator and work package leader and M.Sc. Martina Stavole participates as early stage researcher (ESR10) since 2020.
THREAD addresses the mechanical modelling, mathematical formulations and numerical methods for highly flexible slender structures like yarns, cables, hoses or ropes that are essential parts of high-performance engineering systems. The complex response of such structures in real operational conditions is far beyond the capabilities of current virtual prototyping tools.
This year the second deliverables of two of the main work packages (WP2 and WP3) and the second and third deliverables of WP1 have been successfully submitted. The last project activities, i.e. network-wide training events and secondments, took place. And the project members joined many conferences on-site. Also, the project had a successful third annual meeting on 26-28 September 2022 in Liège, Belgium.


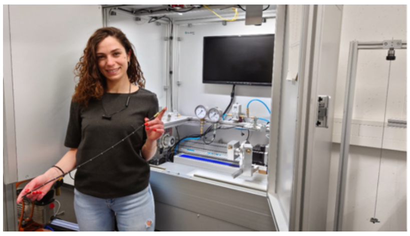

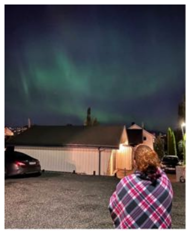

M.Sc. Martina Stavole, successfully completed her planned secondments this year. The aim of the one-month period at ITWM Fraunhofer (Kaiserslautern, Germany) was to test the endoscopes provided by Karl Storz under bending and torsion through MeSOMICS machine. Then, she travelled to Liège (Belgium) to work on the contact problem of the beam with its surrounding. In the end, she completed her last secondment at NTNU in Trondheim (Norway) where she studied quasi-static analyses of a 2D beam in the framework of Neural Networks. More information about the project can be found at https://thread-etn.eu.

3.2 SFB 1483 – EmpkinS

Developing sensor technology and collecting movement data of the human body is the aim of the Collaborative Research Center SFB 1483, which has been approved by the German Research Foundation (DFG) in 2021 for four years. The SFB bears the project title "Empatho-Kinaesthetic Sensor Technology" (EmpkinS) and aims to combine the external observation of body movements, such as movements of the head, torso and limbs, facial expressions with internal processes using body function models to detect several body (dys) functions with non-invasive and in the future easily available sensors. The research team headed by Prof. Dr. Martin Vossiek from the Institute of Microwaves and Photonics and Prof. Dr. Björn Eskofier from the Machine Learning and Data Analytics Lab wants to achieve this by developing methods and technologies that link information from external movements with internal biomedical processes. The external movements are measured with sensory systems, which are also developed within the CRC. EmpkinS focuses on immunology, neurology and palliative medicine as well as mental illnesses such as depression and stress. More information about

the SFB can be found on its website https://www.empkins.de.
Subproject C04 “Analysis of Degenerative Movement Restrictions by Embedding Empathokinesthetic Sensor Data in Biomechanical Human Models” is located at the Institute of Applied Dynamics with principal investigator Prof. Dr.-Ing. habil. Sigrid Leyendecker and M.Sc. Simon Heinrich joined in November 2021 as doctoral candidate.
In close collaboration the subproject D01 “Movement Patterns in Hand Motion from Empathokinesthetic Sensor Data as a Diagnostic Parameter for Disease Activity in Patients with Rheumatic Disease” located at the Department of Internal Medicine 3 – Rheumatology and Immunology started in May 2021. PD Dr. sport science Dr. habil. Anna-Maria Liphardt is working as principal investigator in this project and M.Sc. Birte Coppers as doctoral candidate.
Both subprojects planned and conducted an extensive measurement campaign together. They collected movement data of human hands with the institutes motion capture, electromyography and force measurement systems. The measurements took place at the institute for two months and at the university hospital Erlangen for three months and included 227 participants with different age and sex. The participants were evenly distributed in a control group and two groups with different diseases.
There was an extensive filming campaign to create a general EmpkinS video as well as subpropject specific introduction videos about the work in EmpkinS. These videos will be published on the social media channels of projects to increase the visibility of the CRC. Also, several workshops were realized, both scientific and soft skill based. To name few, there was a Women-of-EmpkinS event, a design your life workshop, a science slam training and a monthly lecture series by the principal investigators. Furthermore, a two-day retreat in February, a five-day retreat (called Winterschool) in November and an additional status seminar for the young researchers were organized. The retreats gave opportunity for intensive discussions about their subprojects, possible joint research questions and to learn about different topics, such as research data management or how to deal with failures.

Group picture of the EmpkinS winterschool in Hintertux.

3.3 FRASCAL – Fracture across Scales

Second cohort of the DFG research training group (RTG) FRASCAL - Fracture across Scales (GRK 2423) started at the beginning of this year (2022). It is a multidisciplinary research training group that involves 12 projects, of which project P9 is being carried out at LTD under the supervision of Prof. Dr.-Ing. habil. Sigrid Leyendecker. During the first cohort of FRASCAL, M.Sc. Dhananjay Phansalkar has successfully developed a variation-based spatially adaptive phase field model of the fracture. Now, in the second cohort, M.Sc. Deepak B. Jadhav is working on the ‘Temporal Adaptivity in the Phase Field model of Dynamic Fracture’ at LTD. This project aims to extend the previously developed spatially adaptive phase field model to incorporate temporal adaptivity in the models of dynamic fractures using asynchronous variational integrators. This research is being carried out in close cooperation with RTG’s Mercator fellow Prof. Dr. Michael Ortiz and Prof. Dr.-Ing. Kerstin

Weinberg from Universität Siegen. The 2nd RTG Retreat of FRASCAL was organised at Arvena Reichsstadt Hotel in Bad Windsheim from May 5 to May 6. The individual presentations and poster blitz event resulted in very productive discussions among the researchers from all groups of the RTG. Also, on 13-14 October RTG organised a two-day autumn school on software development at the Hotel Fuchsbräu in Beilngries, which was very beneficial for all doctoral researchers to enhance their software development skills in C++.


Images by: Dr. Andrea Dakkouri-Baldauf

3.4 Research stay at the Queensland University of Technology (QUT), Australia

For the period from February 2022 to January 2024, Prof. Dr.-Ing. habil. Sigrid Leyendecker has been appointed as an adjunct professor at QUT, a leading Australian university in biomedical engineering. Professor Leyendecker spent her sabbatical semester during the German summer term 2022 at QUT and in particular at the International Training and Transformation Centre for Joint Biomechanics (ITTC-JB), being established at the university campus in 2018. During this time, an international collaboration between FAU and QUT has been intensified and a successful initiation and preparation of an international research training group on musculoskeletal modelling between QUT, FAU, Universitaätsklinikum Erlangen and Technische Hochschule Nürnberg has started. Further, together with Prof. Dr.-Ing. habil. Peter Pivonka from QUT and M. Sc. Denisa Martonová, spending her research stay (April to August 2022) also at QUT, a two-state receptor ligand binding model of parathormon has been newly formulated and implemented and a journal publication has been submitted. In another collaboration project between Professor Leyendecker, M. Sc. Mathhias Schubert and Professor Brown from QUT, a simulation model for the dynamics of small spider webs, based on a geometrically exact string model has been developed.


3.5 SPP 1886

The German Research Foundation (DFG) Priority Programme "Polymorphic uncertainty modelling for the numerical design of structures – SPP 1886" is coordinated by Professor Dr.-Ing. Michael Kaliske from Technische Universität Dresden and Prof. Dr.-Ing. habil. Sigrid Leyendecker is part of the programme committee and principal investigator of one of the projects. In August 2022, the Institute of Applied Dynamics successfully participated in the phase 2 annual meeting in Aachen.

3.6 Dielectric elastomer project

The DFG-Einzelförderung / Sachbeihilfe "Electromechanically coupled beam models for stacked dielectric elastomer actuators" project, initiated last year with Prof. Dr.-Ing. habil. Sigrid Leyendecker as project leader and fellow Dr.-Ing. Dengpeng Huang in the research front. Stacked dielectric elastomer actuators bear analogy to the behaviour of human muscles in terms of contracting in length direction when actuated. They are suitable for point-by-point application of a force. Therefore, dielectric elastomers allow for a sophisticated, efficient and noiseless actuation of systems. However, the use of elastic actuators is also accompanied by new control challenges. As the computational cost for solving optimal control problems is significantly affected by the number of model degrees of freedom, reduced and problem specific actuator models are superior to general but cost-intensive finite element models. To this end, a beam model has been developed in this project for the stacked dielectric elastomer actuators, which has been published in the Journal of Computational Mechanics recently. The application of the beam model in complex multibody system is ongoing.

3.7 Heart project

The heart project is focusing on the modelling of the cardiac function to better understand cardiovascular disease, to be able to early detect or even predict heart failure and develop adequate patient specific therapies and medical devices. We are currently working on a rat as well as a human heart model. In April 2022, a new project entitled Smoothed finite element method in modelling and simulation of cardiac electromechanics funded by German Research Foundation (DFG) has started. The mail goal is to extend an alternative group of numerical techniques, smoothed finite element methods, for cardiac electromechanics to overcome volumetric locking, mesh distortion problem and to decrease simulation time. We are also currently working on a dynamic, viscoelastic, electromechanical shell model to develop an artificial heart muscle to support the cardiac cycle in case of disease.

3.8 Characterisation of Macromolecules

The characterisation of macromolecules project is a cooperation research between the Institute of Applied Dynamics at Friedrich-Alexander-Universität Erlangen-Nürnberg and UCSF Department of Bioengineering and Therapeutic Sciences and is funded by German Research Foundation (DFG). The purpose of this project is characterizing macromolecules e.g. SARS CoV-2 main protease by using the kino-geometric sampling (KGS) method. The rigidity and conformation transition analysis of SARS CoV-2 main protease mutation, will benefit drug development in the SARS CoV-2 field. The project is cooperated by Dr. Henry van den Bedem from Stanford University. M.Sc. Xiyu Chen is focusing on the rigidity analysis and the mutation analysis for SARS CoV-2 main protease binding with different ligands by using the KGS method.

3.9 Scientific reports

The subsequent pages present a brief overview on the current research projects pursued at the Institute of Applied Dynamics. These are partly financed by third-party funding German Research Foundation (DFG), the Klaus Tschira Stiftung, the European Training Network (ETN) and in addition by the core support of the university.

Research topics

Optimal control of a pendulum with set-valued friction
Giuseppe Capobianco, Sigrid Leyendecker

Kinematic analysis of SARS CoV-2 main protease mutation
Xiyu Chen, Sigrid Leyendecker, Henry van den Bedem

Movement Patterns in Hand Motion from Empathokinesthetic Sensor Data as a Diagnostic Parameter for Disease Activity in Patients with Rheumatic Disease
Birte Coppers, Sara Bayat, Arnd Kleyer, Georg Schett, Simon Heinrich, Sigrid Leyendecker, Anna-Maria Liphardt

Development of a dynamic model of the full hand for optimal control simulations
Simon Heinrich, Birte Coppers, Anna-Maria Liphardt, Sigrid Leyendecker

Dielectric shell model as artificial cardiac muscle
David Holz, Dengpeng Huang, Sigrid Leyendecker

Dielectric Elastomer Actuated Multibody System Dynamics and Optimal Control
Dengpeng Huang, Sigrid Leyendecker

Application of the spatially adaptive phase-field model to a splitting test
Deepak Jadhav, Dhananjay Phansalkar, Michael Ortiz, Kerstin Weinberg, Sigrid Leyendecker

Two-state receptor model for dosing patterns of parathyroid hormone
Denisa Martonová, Maxence Lavaill, Mark R. Forwood, Gold Goast, Alexander Robling, David M. L. Cooper, Sigrid Leyendecker and Peter Pivonka

Different convergence concepts for the Newmark algorithm
Dhananjay Phansalkar, Michael Ortiz, Kerstin Weinberg, Sigrid Leyendecker

High order variational integrators for continuum mechanics, constrained mechanical systems and optimal control
Rodrigo T. Sato Martín de Almagro, Sigrid Leyendecker

Modelling soft-tissue artefacts with epistemic uncertainty for knee flexion calculations
Eduard S. Scheiterer, Sigrid Leyendecker

Simulation of spider net dynamics
Matthias Schubert, Sigrid Leyendecker

Experimental campaign for mechanical properties characterization of endoscope shafts
Martina Stavole, Sigrid Leyendecker

Optimal control of a pendulum with set-valued friction

Giuseppe Capobianco, Sigrid Leyendecker

For many engineering applications, friction is vital for their functionality. E.g. for walking and driving, the friction with the ground is exploited for locomotion. The goal of this project is to explore the optimal control of mechanical systems with friction. To do so, as a benchmark problem, we analyze a pendulum driven via a frictional coupling, which exerts a moment M on the pendulum. The moment is due to friction and therefore depends on the difference between the angular velocity of the pendulum $\dot{\varphi}$ and the angular velocity of the driving shaft ω, which is the control input of the system.

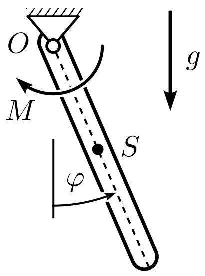

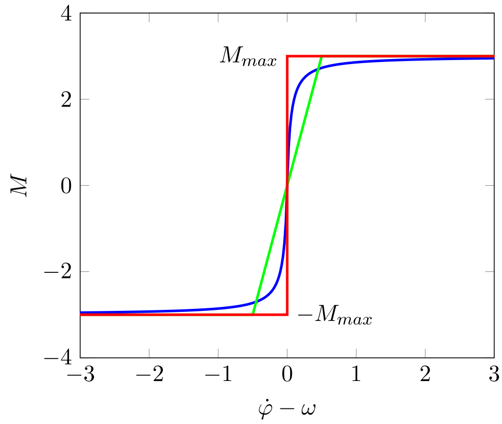

Figure 1: Left: pendulum driven by moment M. Right: Coulomb friction – (red) set-valued, (green) C^0-regularization and (blue) smooth regularization.

To find an upswing trajectory, we solve the optimal control problem of searching the input ω such that starting at rest for $\varphi(0) = 0$, the pendulum swings up to $\varphi(T) = \pi/2$ with $\dot{\varphi}(T) = 0$ and minimizes the cost functional

$$C(\omega) = \frac{1}{2} \int_0^T \omega^2 \mathrm{d}t \,.$$

For the three friction laws shown in Figure 1, an upswing trajectory for $T = 4$ found using the Discrete Mechanics and Optimal Control approach is shown in Figure 2, respectively.

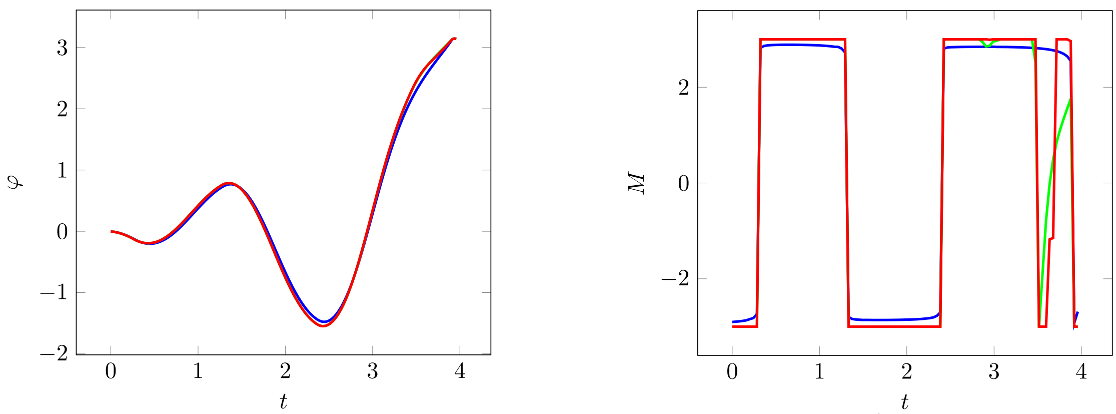

Figure 2: Upswing trajectories with friction law: (red) set-valued, (green) C^0-regularization and (blue) smooth regularization.

The presented results look very promising, however, the convergence behavior of the used method is very parameter sensitive. This stems from the fact that conventional optimization algorithms can barely handle the nonsmooth constraints induced by the friction law. The above results show the need for novel solution strategies, which shall be developed in this prject.

Kinematic analysis of SARS CoV-2 main protease mutation

Xiyu Chen, Sigrid Leyendecker, Henry van den Bedem[1] [2]

In 2019, new coronavirus SARS CoV-2 has emerged and caused a pandemic. The main protease (Mpro) of SARS CoV-2 is known as one of the potential drug targets whose investigation is worthwhile for possible drug development. In particular, Mpro has no human homolog, which decreases the probability to target a wrong host protein and is relatively more safe compared with other targets [1, 2]. However, the influence of the Mpro monomer mutations are still not clear.

Protein flexibility is a significant factor for protein conformation. Moreover, the ligand binding with protein and protein mutation modifies its flexibility. Kinematic flexibility analysis (KFA) is an efficient and fast method to analyze the conformational flexibility and transition of 3D macromolecules and helps us to investigate how their flexibility influences their property. Kinematically, the non-covalent bond, such as hydrogen bonds and hydrophobic interactions, can be modeled as holonomic constraints $\mathbf{\Phi}(\theta)$=$\mathbf{0}$ where all covalent bonds are treated as degrees of freedom θ, see [3, 4]. Consistent with these holonomic constraints, the velocity constraints read as

$$\frac{d\mathbf{\Phi}}{dt} = \mathbf{J}\dot{\theta} = \mathbf{0}$$

Through singular value decomposition of the constraint Jacobian matrix $\mathbf{J} = \frac{\partial \mathbf{\Phi}}{\partial \theta}$, a basis for its nullspace can be determined. The nullspace includes the information of addmissible velocities $\dot{\theta}$ and yields the required information for the molecular rigidity analysis and for conformational transitions.

The Sars CoV2 Mpro is one of the most important drug targets and it is valuable for the study of Sars CoV2 Mpro mutation, we apply the kinematic method to analyze the change in flexibility after the mutation based on the predicted possible mutation sites by O. S. Amamuddy et al. [1]. It includes 47 mutation sites in total: A7, G15, M17, V20, T45, D48, M49, R60, K61, A70, G71, L89, K90, P99, Y101, R105, P108, A116, A129, P132, T135, I136, N151, V157, C160, A173, P184, T190, A191, A193, T196, T198, T201, L220, L232, A234, K236, Y237, D248, A255, T259, A260, V261, A266, N274, R279 and S301L. To investigate the influence of mutation on the Sars CoV2 Mpro binding with different inhibitor ligands, 69 crystal structures binding with different ligands are selected through 100% sequence similarity analysis to crystal structure 6Y2E. The crystal structure 6Y2E is Mpro without ligand binding and the other crystal structures are Mpro binding with one ligand. The root mean squared fluctuation (RMSF) of the atom positions is a good indicator for the flexiblity, which presents the activity and conformational property of Mpro. Fig. 1(A) shows the RMSF value ratio between Mpro with mutation and without mutation for different crystal structures. As shown in Fig. 1, the point below the identity line means the RMSF value is lower and the crystal structures are more flexible after mutation. Most points are under the identity line as shown in Fig. 1(A), so most crystal structures are more flexible after mutation. More flexible crystal structures indicates the crystal structure has higher entropy and lower free energy, and for the Sars CoV2 Mpro, the crystal structure is more stable after the mutation and binding stronger with ligand. Fig. 1(B) shows the RMSF value ratio between Mpro with ligand to without ligand binding for different crystal structures after mutation. Only two crystal structures are more flexible after binding with a ligand, the other crystal structures are more rigidified after binding with ligands. Fig. 1(C) shows the the ratio of rigidified DoFs to cycle DoFs for all 47 single mutation sites. the Mpro crystal structures are more flexible after mutation compared to without mutation.

[1] Atomwise, Inc. 717 Market Street, San Francisco, CA 94103 USA
[2] Department of Bioengineering and Therapeutic Sciences, UCSF, California, USA

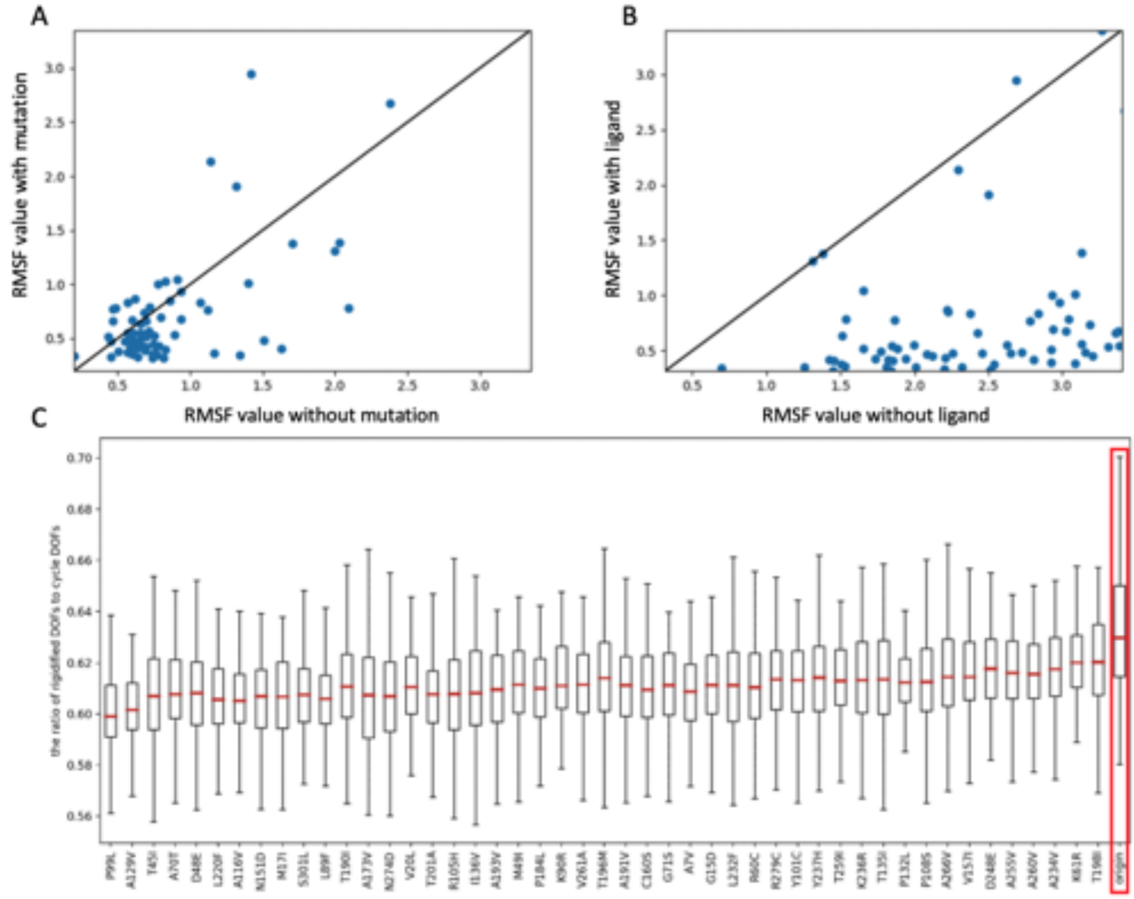

Figure 1: SARS CoV-2 Mpro mutation analysis based on the kinematical method. (A) the root mean square fluctuation RMSF value ratio between Mpro with mutation to without mutation for different crystal structures (B) the RMSF value ratio between Mpro with ligand to without ligand binding for different crystal structures (C) the ratio of rigidified DoFs to cycle DoFs for different single mutation sites

References

[1] O. S. Amamuddy, Gennady M. Verkhivker and Ö. T. Bishop. Impact of emerging mutations on the dynamic properties the SARS-CoV-2 main protease: an in silico investigation. Journal of Chemical Information and Modeling. 2021

[2] S. Chen et al. Mutation of Gly-11 on the Dimer Interface Results in the Complete Crystallographic Dimer Dissociation of Severe Acute Respiratory Syndrome Coronavirus 3C-like Protease. Journal of Biological Chemistry. 283, 554-564, 2008

[3] D. Budday, S. Leyendecker, and H. van den Bedem. Kinematic Flexibility Analysis: Hydrogen Bonding Patterns Impart a Spatial Hierarchy of Protein Motion. Journal of Chemical Information and Modeling 58(10), 2108-2122, 2018

[4] X. Chen, S. Leyendecker, H. van den Bedem. Kinematic Flexibility Analysis of Active and Inactive Kinase Conformations Proceedings in Applied Mathematics and Mechanics, 2020

Evaluation and perspectives of using marker-based motion capturing to characterize hand movements in patients with rheumatic diseases

B. Coppers[1], S. Bayat[1], A. Kleyer[1], G. Schett[1], S. Heinrich, S. Leyendecker, A.M. Liphardt[1]

The analysis of hand motion is challenging due to the high complexity of the hand including more than 25 degrees of freedom [1]. Functional impairment of the hand is characteristic [3] for patients with rheumatoid arthritis (RA) and monitoring function in is essential for effective treatment [5] in this patient group. Hand movement patterns may provide new possibilities for the assessment of quantitative and qualitative changes of hand function in relation to disease activity in RA patients [4]. Anatomic and empirical studies of healthy individuals revealed that e.g. movement of the distal interphalangeal joint (DIP) and proximal interphalangeal joint (PIP) is related with an almost linear relationship [7]. In this data analysis we aimed to examine if (a) the DIP/PIP ratio extracted from a passive marker-based optoelectronic measurement system (OMS), applies to RA patients and (b) differences in the DIP/PIP ratio can discriminate between RA patients and healthy controls (HC).
Twenty-four patients with RA (ACR/EULAR 2010 criteria [2]recruited from the Internal Medicine 3 outpatient clinics, Erlangen, Germany and 23 HC participated in this pilot study [6]. Participants were asked to flex the DIP and PIP joints of both hands for three times, starting with an open hand posture Fig. (1).Hand segment movement was captured using an OMS (eight Oqus7+ cameras and one Oqus5+ camera, Qualisys AB, Sweden) at a frame rate of 100 Hz with a set of 29 retroreflective markers placed on the hand dorsum [1] . The ratio between the flexion angle of the DIP and PIP joint were calculated for each finger using an approach previously described by Sancho-Bru et al. (2014) as well as the linear fit (R2).

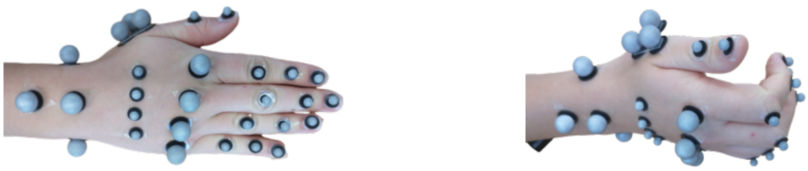

Figure 1: Marker-setup for extension – flexion movement of DIP and PIP joints.

The overall angle ratio for both groups was affected by sex, showing an 8% lower ratio for women (95% CI -15% to -1%). Measured angle ratios (RA 0.60 $\pm$ 0.15; HC 0.68 $\pm$ 0.17 (DIP/PIP)) and their linear fit (RA 0.96 $\pm$ 0.05; HC 0.97 $\pm$ 0.03 R2) were similar for RA and controls ($p > 0.05$).

This analysis highlighted that the previously described linear relationship of angle ratios for the distal finger joints in healthy individuals [7]] is also valid for RA patients in this cohort. Variation for the value of the ratio could only be explained by sex-specific differences and no significant group differences between RA und HC were identified. Sex differences are a common phenomenon in functional tests that need to be considered [4]. Also, this may reflect that DIP and PIP joints are less affected in RA compared to other inflammatory arthritic diseases, e.g. psoriatic arthritis [5].
In 2022 an extensive study took place in order to assess hand movements in rheumatic diseases compared with healthy study participant across different ages and between men and women (Fig. 3). We included three groups of people in this study - 73 patients with rheumatoid arthritis, 77 patients with psoriatic arthritis and 76 healthy controls in equally balanced age (between 20 - 80+ years) and

[1]Department of Internal Medicine 3 – Rheumatology and Immunology, Universitätsklinikum, Friedrich-Alexander-Universität Erlangen-Nürnberg, Ulmenweg 18, D-91054 Erlangen, Germany

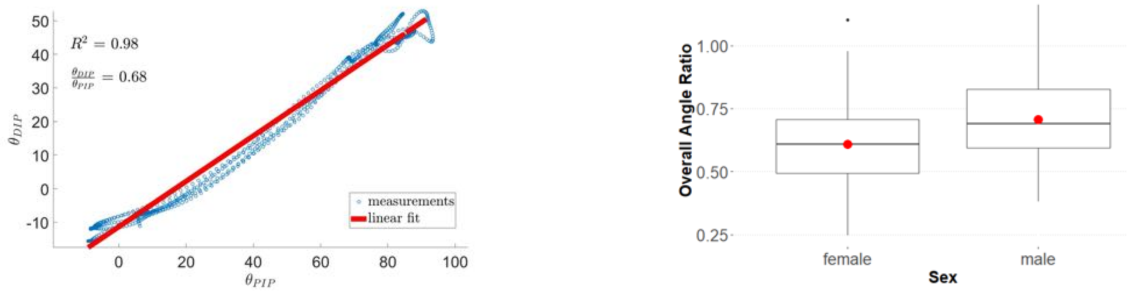

Figure 2: left: DIP/PIP angle ratio, measured values, linear fit and R2 for the little finger of one RA patient, right: overall mean, quantiles, maximum and minimum DIP/PIP angle ratio by sex (p¡0.05).

sex groups. Based on this study we are aiming to identify hand movement characteristics that are typical for either of the three groups.

Figure 3: Different movement tasks.

Acknowledgments This work was funded by the Deutsche Forschungsgemeinschaft (DFG, German Research Foundation) – SFB 1483 – Project-ID 442419336, EmpkinS.

References

[1] Sancho-Bru, J. L., Jarque-Bou, N. J., Vergara, M., and Pérez-González, A. (2014) *Validity of a simple videogrammetric method to measure the movement of all hand segments for clinical purposes.* Proc Inst Mech Eng H. **228(2)**, 182–189(2014).

[2] Aletaha, D., et al . *Rheumatoid arthritis classification criteria: an American College of Rheumatology/European League Against Rheumatism collaborative initiative.* Arthritis Rheum. **62(9)**, 2569-81 (2010).

[3] Günay, S. M., et al. *Relationship between patient-reported and objective measurements of hand function in patients with rheumatoid arthritis.* Reumatismo. **68(4)**, 183-187 (2016).

[4] Liphardt, A.M.; Manger, E.; Liehr, S.; Bieniek, L.; Kleyer, A.; Simon, D.; Tascilar, K.; Sticherling, M.; Rech, J.; Schett, G.; et al. (2020). *Similar impact of psoriatic arthritis and rheumatoid arthritis on objective and subjective parameters of hand function.* ACR Open Rheumatol. **2(12)**, 734–740(2020).

[5] Veale, D. J., and Fearon, U. (2015). *What makes psoriatic and rheumatoid arthritis so different?* RMD Open . **1(e000025)**.

[6] Phutane, U., Liphardt A.M., Bräunig J., et. al. *Evaluation of Optical and Radar Based Motion Capturing Technologies for Characterizing Hand Movement in Rheumatoid Arthritis-A Pilot Study.* Sensors (Basel) **21(4)**, 1208(2021).

[7] Rijpkema, H. G., Michael. (1991). *Computer Animation of Knowledge-Based Human Grasping.* Computer Graphics **24(4)**.

Development of a dynamic model of the full hand for optimal control simulations

Simon Heinrich, Birte Coppers[1,2], Anna-Maria Liphardt[1,2], Sigrid Leyendecker

Dynamic simulations of human hands can be used to obtain insight in non-observable quantities in the hand during motion. Such quantities are constraint forces in the joints, actuation torques, stresses in bones, and muscle forces and activation. One approach to simulate realistic motions is to use optimal control simulations, where a physiologically motivated objective function is minimized while the state of the model is influenced by control variables. The optimal control problem also contains constraints accounting for the models' dynamics, boundary constraints for the initial and final state and constraints on the evolution of the variables, so-called path constraints. The objective function can be, for example, the maximum torque or force, the change in torque or force over time, the time to perform the task, or a combination of several quantities [1].
We model the hand as a system of rigid bodies, with simplified geometry and constant density. Multiple bodies are connected by ideal joints. These joints also constrain the motion between connected bodies. Here, we use revolute joints, cardan joints and nino joints. The latter are joints with two axes of rotation that are non-intersecting and non-orthogonal. They are proposed for the thumb by [2] and were used and validated for a thumb model by [3]. The complete structure of the hand, with its degrees of freedom in each joint can be seen in Fig. 1. The pose of the whole model, with its N bodies is then described in redundant coordinates $\boldsymbol{q} = \left((\boldsymbol{q}^1)^T \quad \dots \quad (\boldsymbol{q}^N)^T\right)^T \in \mathbb{R}^{12N}$. These coordinates are constrained to depict the rigid body motion of the system.
We formulate the optimal control problem and solve it within the frame of discrete mechancis and optimal control (DMOCC) [4]. To derive the equations of motion we start with a Lagrangian of the mechanical system $L(\boldsymbol{q}, \dot{\boldsymbol{q}}) = T(\dot{\boldsymbol{q}}) - V(\boldsymbol{q})$, with the kinetic energy T and the potential energy V. The constrained Lagrangian also includes the constraints of the system $\boldsymbol{g}(\boldsymbol{q})$ and a Lagrange multiplier $\boldsymbol{\lambda}$. Its action is defined as the integral of the Lagrangian over time and is approximated by means of a discrete constrained Lagrangian L_d in Eq. (1). Finding stationary points for the discrete action sum $S_d = \sum_{n=0}^{T-1} L_d(\boldsymbol{q}_n, \boldsymbol{q}_{n+1})$, meaning the variation of S_d vanishes, provides us with the discrete Euler-Lagrange equations. Using a nullspace matrix $\boldsymbol{P}(\boldsymbol{q})$ eliminates the constraint forces and leads to the projected discrete Euler-Lagrange equations in Eq. (2). D_i denotes a derivation with respect to the i-th variable.

$$L_d(\boldsymbol{q}_n, \boldsymbol{q}_{n+1}) \approx \int_{t_n}^{t_{n+1}} L(\boldsymbol{q}, \dot{\boldsymbol{q}}) - \boldsymbol{g}^T(\boldsymbol{q}) \cdot \boldsymbol{\lambda} dt \tag{1}$$

$$\boldsymbol{P}^T(\boldsymbol{q}) \cdot \left(D_1 L_d(\boldsymbol{q}_n, \boldsymbol{q}_{n+1}) + D_2 L_d(\boldsymbol{q}_{n-1}, \boldsymbol{q}_n)\right) = 0 \tag{2}$$

Additionally, introducing approximations of the acting forces $\boldsymbol{f}_n^{\pm}$ and a reparametrization of the pose at the unknown timestep $n+1$ with an incremental update $\boldsymbol{u}_{n+1}$ $\boldsymbol{q}_{n+1} = \boldsymbol{F}_d(\boldsymbol{u}_{n+1}, \boldsymbol{q}_n)$ as in [4] gives the projected Euler-Lagrange equations with forces in Eq. (3). They can be used for optimal control simulations, as well as forward and inverse dynamic simulations.

$$\boldsymbol{P}^T(\boldsymbol{q}) \cdot \left(D_1 L_d(\boldsymbol{q}_n, \boldsymbol{F}_d(\boldsymbol{u}_{n+1}, \boldsymbol{q}_n)) + D_2 L_d(\boldsymbol{q}_{n-1}, \boldsymbol{q}_n) + \boldsymbol{f}_{n-1}^{+} + \boldsymbol{f}_n^{-}\right) = 0 \tag{3}$$

Using this framework has several desired properties, namely preservation of the underlying structure of the mechanical system, the preservation of symplecticity, the good energy behavior over exponentially

[1]Department of Internal Medicine 3 – Rheumatology and Immunology, University Clinic Erlangen, Friedrich-Alexander-Universität Erlangen-Nürnberg, Ulmenweg 18, D-91054 Erlangen, Germany
[2]Deutsches Zentrum für Immuntherapie, University Clinic Erlangen, Friedrich-Alexander-Universität Erlangen-Nürnberg, Ulmenweg 18, D-91054 Erlangen, Germany

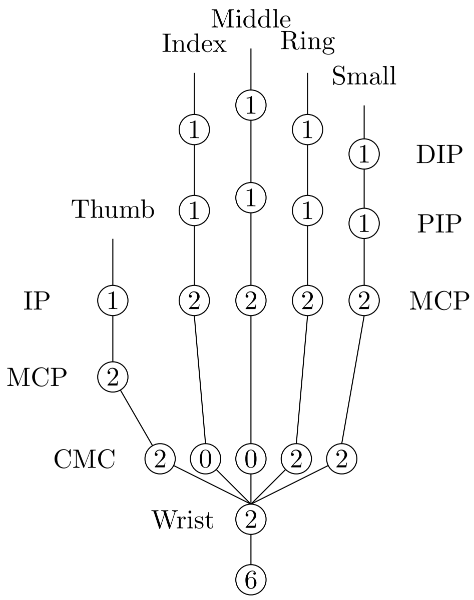

Figure 1: Structure of the hand model. Lines denote bodies and circles denote joints with the degrees of freedom written inside them.

long times and the preservation of momentum maps. This allows to choose larger time steps while still obtaining physically meaningful results.
The optimal control simulations can be now written as a constrained optimization problem as in Eq. (4), where J_d is a discrete functional accounting for any measure of optimality.

$$\begin{aligned} & \min_{\boldsymbol{u}_d, \boldsymbol{f}_d^+, \boldsymbol{f}_d^-} \sum_{n=0}^{T-1} J_d(\boldsymbol{q}_n, \boldsymbol{F}_d(\boldsymbol{u}_{n+1}, \boldsymbol{q}_n), \boldsymbol{f}_d^+, \boldsymbol{f}_d^-) \\ \text{subject to} \quad & \text{system dynamics Eq. (3)} \\ & \text{boundary constraints} \\ & \text{path constraints} \end{aligned} \tag{4}$$

Acknowledgements This work was supported by the Deutsche Forschungsgemeinschaft (DFG, German Research Foundation) under Grant SFB 1483–Project-ID 442419336.

References

[1] Maas, R; *Biomechanics and optimal control simulations of the human upper extermity.* Friedrich-Alexander Universität Erlangen-Nürnberg, 2014

[2] Hollister, A. et al: *The Axes of Rotation of the Thumb Carpometacarpal Joint.* J. Orthop. Res., 1992.

[3] Phutane, U. et al: *Kinematic validation of a human thumb model.* ECCOMAS - Thematic Conference on Multibody Dynamics, 2017

[4] Leyendecker, S: *On optimal control simulations for mechanical systems.* Technische Universität Kaiserlautern, 2011.

Dielectric shell model as artificial cardiac muscle

David Holz, Dengpeng Huang, Sigrid Leyendecker

Nowadays, the properties of dielectric elastomer actuators are beneficial in a variety of applications, e.g. artificial muscle actuators in soft robotics, diaphragm actuators for pumps or acoustic loudspeakers. In this work, a dynamic, viscoelastic artificial cardiac muscle model (structural element shell; Mindlin-Reissner shell kinematics) based on a dielectric material is developed. The model is based on the shell formulation in [1] and the electromechanically coupled beam formulation in [2]. This artificial cardiac muscle has a support function during the systolic and diastolic phase of the cardiac cycle, see also [3]. A thin-walled layer of the dielectric material surrounding the heart represents the artificial cardiac muscle, see Fig. 1. The volume between the artificial muscle model and the heart is assumed to be filled with an incompressible fluid.

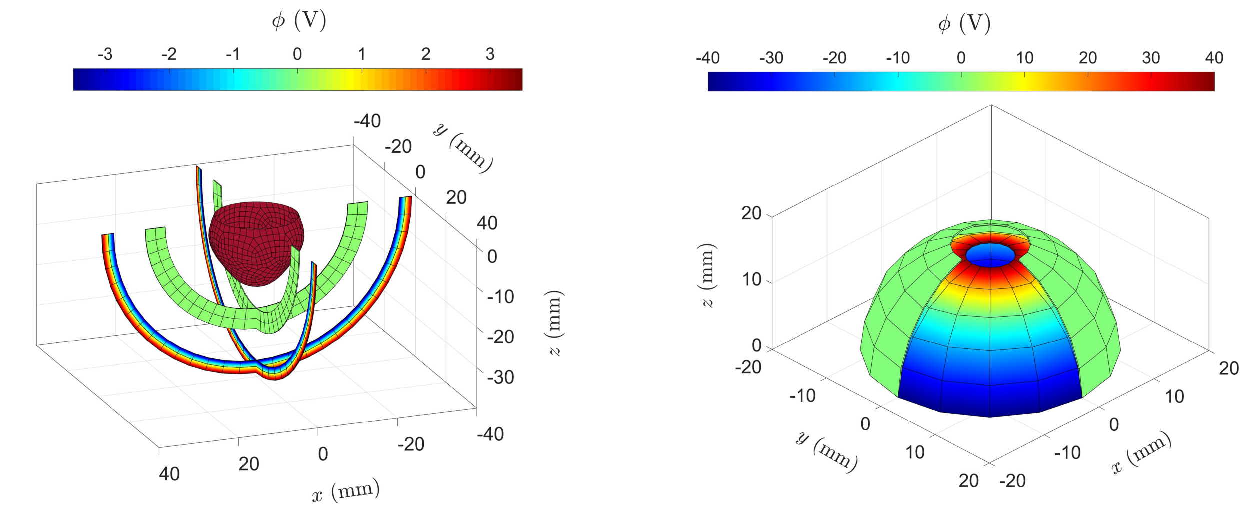

Figure 1: On the left, a dummy heart model is depicted surrounded by the artificial muscle model in the undeformed and deformed configuration. Depending on the applied voltage ϕ, the artificial muscle deforms and is capable of generating a positive or negative pressure on the pericardium of the heart. On the right, a 3D model of the artificial muscle in the undeformed and deformed configuration is visualised.

In the next steps, the model can be extended by allowing thickness strains of the shell and the coupling with an electromechanical finite element model of the heart via a pressure boundary condition.

References

[1] J. C. Simo, D. D. Fox. *On a stress resultant geometrically exact shell model. Part I: Formulation and optimal parametrization.* Computer Methods in Applied Mechanics and Engineering **72:3**, 267–304 (1989).

[2] D. Huang, S. Leyendecker. *An electromechanically coupled beam model for dielectric elastomer actuators.* Computational Mechanics **69:3**, 805–824 (2022).

[3] D. Martonová, D. Holz, D. Brackenhammer, M. Weyand, S. Leyendecker, M. Alkassar. *Support Pressure Acting on the Epicardial Surface of a Rat Left Ventricle–A Computational Study.* Frontiers in Cardiovascular Medicine **9**, (2022).

Dielectric Elastomer Actuated Multibody System Dynamics and Optimal Control

Dengpeng Huang, Sigrid Leyendecker

In this work, a simulation model for the optimal control of dielectric elastomer actuated flexible multibody dynamical systems is presented. The Dielectric Elastomer Actuator (DEA) behaves like a flexible artificial muscle in soft robotics. It is modeled as an electromechanically coupled geometrically exact beam, where the electric charges serve as control variables. The DEA-beam is integrated as an actuator into multibody systems consisting of rigid and flexible components. The model also represents contact interaction via unilateral constraints between the beam actuator and a rigid body. The electromechanically coupled geometrically exact beam is firstly semidiscretized with 1D finite elements and then the multibody dynamics is temporally discretized with a variational integrator leading to the discrete Euler-Lagrange equations.

Optimal control of DEA actuated multibody dynamics

The variational formulation of the electomechanically coupled multibody dynamics problem is based on the Lagrange-d'Alembert principle

$$\delta \int_0^T \left[L(\mathbf{q},\dot{\mathbf{q}}) - \mathbf{g}^T(\mathbf{q}) \cdot \boldsymbol{\lambda} - \mathbf{g}^{cT}(\mathbf{q}) \cdot \boldsymbol{\lambda}^c \right] dt + \int_0^T \mathbf{f}^{ext}(t) \cdot \delta \mathbf{q} dt = 0,$$

where the configuration $\mathbf{q} = \begin{bmatrix} \boldsymbol{\varphi} & \mathbf{d}_1 & \mathbf{d}_2 & \mathbf{d}_3 & \boldsymbol{\phi} \end{bmatrix}^T$ contains the mechanical and electrical degrees of freedom, the external force $\mathbf{f}^{ext} = \begin{bmatrix} \mathbf{f}^v(\mathbf{q},\dot{\mathbf{q}}) & \mathbf{Q} \end{bmatrix}^T$ contains the damping force $\mathbf{f}^v$ and the electric charge $\mathbf{Q}$. The holonomic constraints are represented with $\mathbf{g}$. The contact constraints are complemented with the Kuhn–Tucker conditions $\mathbf{g}^c(\mathbf{q}) \geqslant 0, \boldsymbol{\lambda}^c \leqslant 0, \mathbf{g}^c(\mathbf{q}) \cdot \boldsymbol{\lambda}^c = 0$. The Lagrangian L is given as the difference between the kinetic energy T and internal potential energy V, i.e. $L(\mathbf{q},\dot{\mathbf{q}}) = T(\dot{\mathbf{q}}) - V(\mathbf{q})$ with $V(\mathbf{q}) = \int_c \Omega^b ds$, where the coupled strain energy density Ω^b for the DEA beam is formulated in terms of the mechanical strains $(\boldsymbol{\Gamma}, \mathbf{K})$ and the electrical strains $(\boldsymbol{\Xi}, \boldsymbol{\Theta})$ as [1],

$$\begin{aligned}\Omega^b(\boldsymbol{\Gamma},\mathbf{K},\boldsymbol{\Xi},\boldsymbol{\Theta}) = &\underbrace{\frac{1}{2}\boldsymbol{\Gamma}^T\mathbf{D}_1\boldsymbol{\Gamma} + \frac{1}{2}\mathbf{K}^T\mathbf{D}_2\mathbf{K}}_{mechanical} + \underbrace{(c_1+c_2)\boldsymbol{\Xi}^T\mathbf{D}_3\boldsymbol{\Xi} + (c_1+c_2)\boldsymbol{\Xi}^T\mathbf{D}_4\boldsymbol{\Theta}}_{electrical} \\ &+ \underbrace{2c_2\Xi_3\boldsymbol{\Xi}^T\boldsymbol{\Gamma} + 2c_2\Gamma_3(\Theta_1^2 I_1 + \Theta_2^2 I_2)}_{\boldsymbol{\Xi},\boldsymbol{\Theta}\, coupled\, with\, \boldsymbol{\Gamma}} + \underbrace{2c_2K_3(\Xi_2\Theta_1 I_1 - \Xi_1\Theta_2 I_2) + 4c_2\Xi_3(\Theta_2K_1I_2 - \Theta_1K_2I_1)}_{\boldsymbol{\Xi},\boldsymbol{\Theta}\, coupled\, with\, \mathbf{K}}.\end{aligned}$$

The optimal control problem is formulated as the constrained optimisation in terms of variable $\mathbf{x} = \begin{bmatrix} \mathbf{q} & \boldsymbol{\lambda}^c & \mathbf{Q} \end{bmatrix}$

$$\underset{x}{min}\ J(\mathbf{x})$$

such that the Euler-Lagrange equations, the boundary conditions and the complementary conditions are satisfied (see the formulations in [2]). As an example for the control objective, the change of electric potential over time is applied in this work, i.e. $J(\mathbf{x}) = \dot{\boldsymbol{\phi}}$.

Numerical Examples

The first example is the optimal control of a soft robotic worm, where two rigid cubes are connected to an electromechanically coupled beam via revolute joints. The beam is set to be straight in the initial state and bent in the final state. In the simulation, the two cubes are fixed in the z-direction. First, the optimal trajectories of electric potential (yielding an objective value of $J = 1.33 \times 10^{-13}$) are obtained by solving the constrained optimization problem. Then, the electric potential is applied as boundary conditions in the forward dynamics simulation as shown in Fig. 1, where two phases of motion, the actuated bending (optimal control problem) and the free stretching (forward dynamics) are simulated. A Heaviside type friction law is imposed on both rigid cubes such that the worm can only march forward. With this, one can see how the worm moves forward.

The second example is the optimal control of a soft two-finger grasping robot, where two electromechanically coupled beams represent soft robotic fingers that grasp a rigid cylinder. The two fingers are totally fixed at the bottom and are initially in straight and steady state. As the final condition, only the final position of the

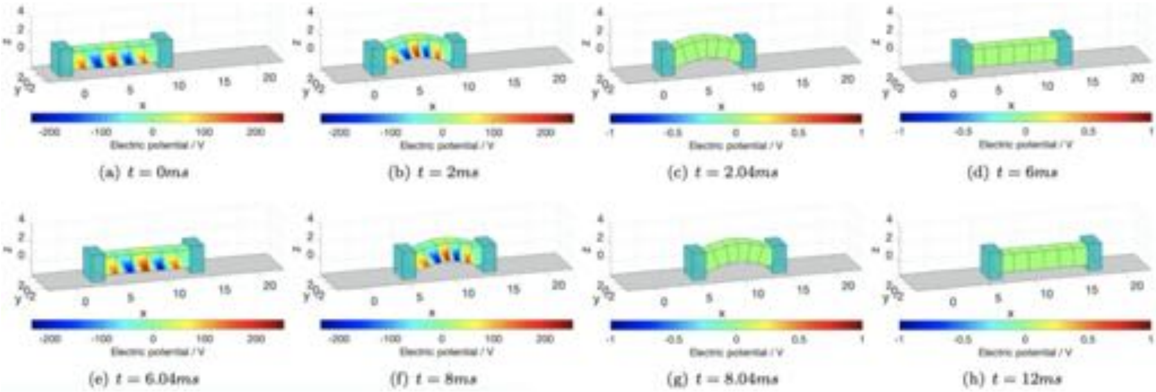

Figure 1: Configurations of the soft robotic worm.

cylinder is constrained whereas the final state for the beams are not constrained, which leads to a grasp in which the optimization determines where the contact shall be closed. The optimised grasping process is shown in Fig. 2. As required in the control objective, the constant electric potential over time is maintained. The electric charges on the last two nodes of the 5-cell-beam is shown in Fig. 3.

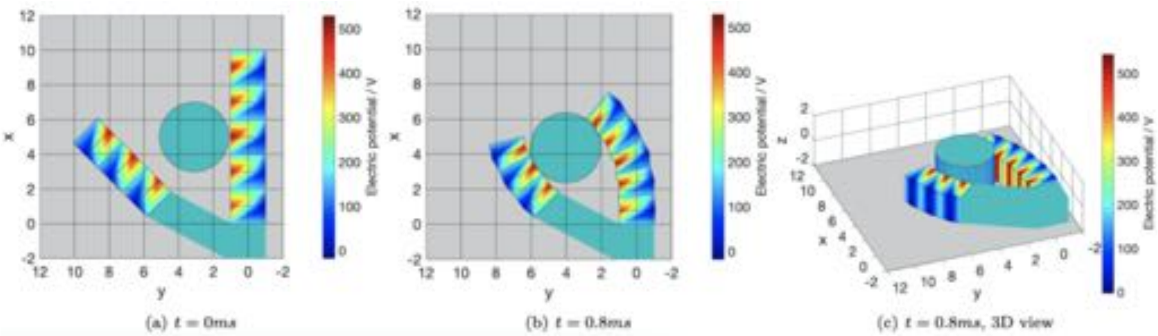

Figure 2: Configurations of the soft robotic grasper (Turquoise bodies are rigid).

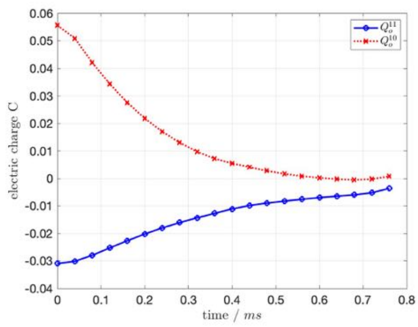

Figure 3: Electric charges on the last two nodes of the 5-cell-beam.

References

[1] D. Huang, S. Leyendecker. An electromechanically coupled beam model for dielectric elastomer actuators. Computational Mechanics, 69(2022)(3):805-824.

[2] D. Huang and S. Leyendecker. Optimal control of dielectric elastomer actuated multibody dynamical systems. arXiv:2207.06424, (2022).

Application of the spatially adaptive phase-field model to a splitting test

Deepak Jadhav, Dhananjay Phansalkar, Michael Ortiz[1], Kerstin Weinberg[2], Sigrid Leyendecker

In fracture mechanics, there are two primary computational modelling strategies: discrete and diffusive crack approaches. Generally, the discrete crack strategies are complex to implement and computationally expensive. On the other hand, the diffusive crack approach is easy to implement by using standard finite element libraries. The diffusive crack approach has been broadly studied and reported in publications for different material models and complex applications[4, 5]. It is based on the regularization length parameter ϵ under the condition that $h << \epsilon$, where h is the mesh size. Hence, to resolve the small length parameter ϵ, very fine meshes are needed which may cause high computational costs.

This issue was addressed by interpreting ϵ as a field variable [1] modifying the energy function used in the standard phase field model [2]. We extend the spatially adaptive phase field model [1] by employing the strain energy split [3] to guarantee only tensile strain energy drives crack propagation. This results in an energy functional given as

$$E(\boldsymbol{u}, c, \epsilon) = \int_{\Omega} [1-c]^2 \psi^+(\boldsymbol{\varepsilon}) + \psi^-(\boldsymbol{\varepsilon}) + \mathcal{G}_c \left[\frac{c^2+\eta}{2\epsilon} + \frac{\epsilon}{2} |\nabla c|^2 \right] + \beta \epsilon \, \mathrm{d}\boldsymbol{x} \tag{1}$$

where $\boldsymbol{u}(\boldsymbol{x})$ is the displacement and $c(\boldsymbol{x})$ the phase-field; $\boldsymbol{\varepsilon} = \mathrm{sym}(\nabla \boldsymbol{u}(\boldsymbol{x})))$ represents the strain tensor, $\epsilon(\boldsymbol{x})$ is the regularisation length variable, β and η are penalty and model parameter respectively, and the strain energy $\psi(\boldsymbol{\varepsilon})$ is split into tensile $\psi^+(\boldsymbol{\varepsilon})$ and compressive $\psi^-(\boldsymbol{\varepsilon})$ parts according to [3]. Minimizing the above mentioned energy functional with respect to $\boldsymbol{u}(\boldsymbol{x}), c(\boldsymbol{x})$ and $\epsilon(\boldsymbol{x})$ leads to the following Euler-Lagrange equations,

$$\mathrm{DIV}[[1-c]^2 \boldsymbol{\sigma}^+ + \boldsymbol{\sigma}^-] = \mathbf{0} \quad \text{in} \quad \Omega \tag{2}$$

$$\frac{c\mathcal{G}_c}{\epsilon} - 2\,[1-c]\,\psi^+(\boldsymbol{\varepsilon}) - \mathcal{G}_c \nabla \cdot [\epsilon \nabla c] = 0 \quad \text{in} \quad \Omega \tag{3}$$

$$\epsilon = \sqrt{\frac{c^2+\eta}{|\nabla c|^2 + \frac{2\beta}{\mathcal{G}_c}}} \quad \text{in} \quad \Omega \tag{4}$$

In these equations, tensile and compressive stresses are expressed by $\boldsymbol{\sigma}^+$ and $\boldsymbol{\sigma}^-$ respectively. These equations are then solved in combination with the boundary conditions $\boldsymbol{u} = \boldsymbol{u_0}$ on $\partial\Omega_{\mathrm{d}}$, $c = c_0$ on $\partial\Omega_{\mathrm{p}}$, and $\nabla c \cdot \boldsymbol{n} = 0$ on $\partial\Omega \setminus \partial\Omega_{\mathrm{p}}$ with the outward normal of the mesh $\boldsymbol{n}$.

Previously, the spatially adaptive phase-field model was employed to study single-edge notch tension specimen [1]. We have extended this model to investigate fracture in a splitting test specimen. The specimen is a rectangular plate with an initial notch, as shown in Figure 1. It is composed of two regions, region 1 and region 2, which have a critical energy release rate $\mathcal{G}_c = 2.70$ MPa mm and $\mathcal{G}_c = 0.54$ MPa mm, respectively. However, we have employed the same Lamé parameters $\mu = 80.7692 \cdot 10^3$ MPa, $\lambda = 121.1538 \cdot 10^3$ MPa for both the regions. The boundary conditions are as illustrated in Figure 1.

Due to the fact that the fracture energy varies between the two regions, the parameters η and β are calculated separately for each zone in accordance with [1]. The parameters used in the simulation are $\eta_1 = 0.6875$, $\beta_1 = 29.0039$, $\eta_2 = 0.6875$, and $\beta_2 = 145.0195$. The simulation is performed by applying a monotonically increasing displacement in increments of $\Delta u = 1 \cdot 10^{-5}$ mm to the splitting test specimen. Figure 2 compares the computed force vs. displacement curves for the spatially varying length variable $\epsilon(\boldsymbol{x})$ to those of a given constant $\epsilon = 0.08$ with an intial mesh size $h = 0.04$ and $h = 0.005$. It demonstrates that the adaptive phase-field model is capable of producing a superior outcome or a result equivalent to a fine mesh while starting with a very coarse mesh. Figure 3 depicts the distribution of the $\epsilon(\boldsymbol{x})$ field and mesh refinement at the crack tip in

[1]Division of Engineering and Applied Sciences, California Institute of Technology, California, USA
[2]Lehrstuhl für Festkörpermechanik, Universität Siegen, 57076 Siegen, Germany

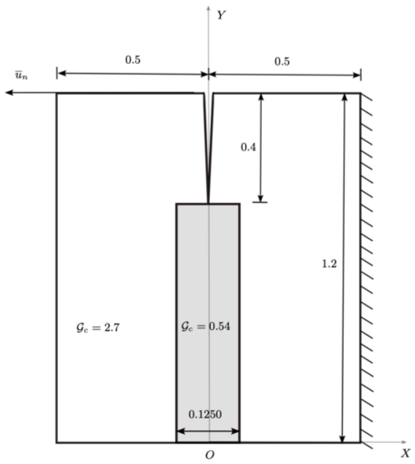

Figure 1: Geometry and boundary conditions for the splitting test

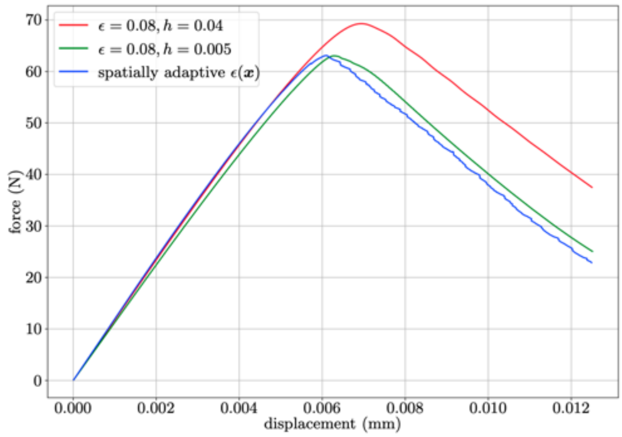

Figure 2: Force vs. displacement plot for the splitting test

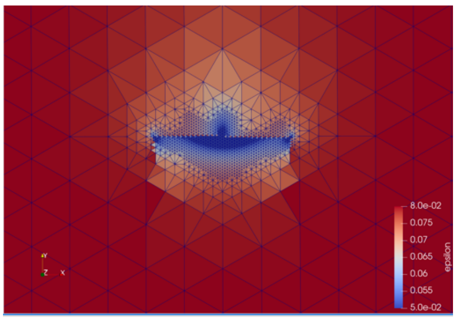

Figure 3: Mesh refinement at $\overline{u}_n = 0.00002$ and contour plot for the length variable $\epsilon(\boldsymbol{x})$ near the crack tip; blue and red regions represent small and large values of ϵ, respectively

the spatially adaptive phase-field model. In the future, we will include temporal adaptation into the spatially adaptive phase field model and employ it to investigate the dynamic brittle fracture in greater depth.

Acknowledgement: This research was funded by the Deutsche Forschungsgemeinschaft (DFG, German Research Foundation) - 377472739/GRK 2423/1-2019. The authors are very grateful for this support.

References

[1] D. Phansalkar, K. Weinberg, M. Ortiz, Michael and S. Leyendecker. *A spatially adaptive phase-field model of fracture.*, Computer Methods in Applied Mechanics and Engineering, 395, 114880, 2022.

[2] A. Giacomini. *Approximation of Quasi-Static Evolution of Brittle Fractures.* Calculus of Variations and Partial Differential Equations, 22:129–172, 2005.

[3] H. Amor, J.-J. Marigo, C. Maurini. *Regularized formulation of the variational brittle fracture with unilateral contact: Numerical experiments.* Journal of the Mechanics and Physics of Solids, 57,1209–1229, 2009.

[4] C. Miehe, F. Welschinger and M. Hofacker. *Thermodynamically consistent phase-field models of fracture: Variational principles and multi-field FE implementations.* INTERNATIONAL JOURNAL FOR NUMERICAL METHODS IN ENGINEERING, 83:1273–1311, 2010.

[5] M. Ambati, T. Gerasimov, Laura De Lorenzis. *A review on phase-field models of brittle fracture and a new fast hybrid formulation.* Computational Mechanics, 55:383–405, 2014.

Two-state receptor model for dosing patterns of parathyroid hormone

Denisa Martonová, Maxence Lavaill[1], Mark R. Forwood[2], Alexander Robling[3], David M. L. Cooper[4], Sigrid Leyendecker, Peter Pivonka[1]

Temporal aspects of ligand specificity have been shown to play a significant role in the case of pulsatile hormone secretion, such as parathyroid hormone (PTH) binding to its receptor (PTH1R). We utilise a two-state receptor ligand binding model of PTH to PTH1R, first proposed by Segel et al. [1], in order to investigate the cellular responsiveness α_R in healthy and pathological cases.

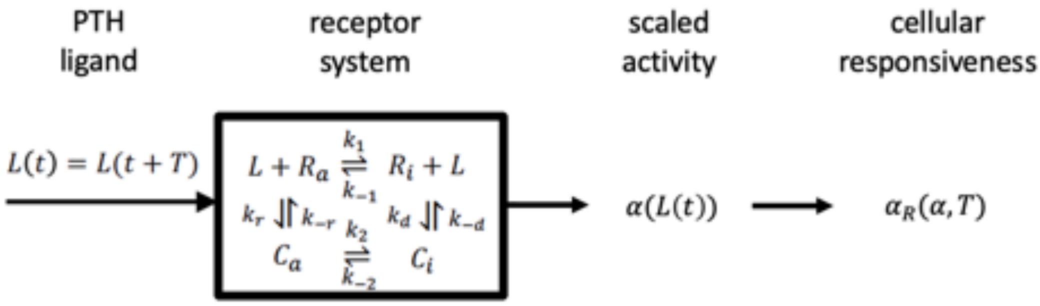

Figure 1: Schematic of the two-state receptor model representing PTH to PTH1R binding [1].

PTH1R can change conformation independent of a ligand, namely from its active state R_a to the inactive state R_i and vice versa. Both receptor states combined with the PTH ligand L form active and inactive ligand-receptor complexes C_a and C_i, respectively (see Fig 1 for a schematic of the model kinetics). This creates a distribution among the four receptor species with the total concentration of receptor $R_T(= [R_a] + [C_a] + [C_i] + [R_i])$. The ordinary differential equation for the two-state receptor model can be summarised in matrix notation as [2]

$$\frac{d\mathbf{C}}{dt} = \mathbf{K}(L(t))\mathbf{C}(t), \tag{1}$$

where the vector of unknown concentration $\mathbf{C}$ for the receptor states and the constant coefficient matrix $\mathbf{K}$ describing the ligand-receptor binding kinetics are given as

$$\mathbf{C} = \begin{bmatrix} r_a \\ c_a \\ c_i \\ r_i \end{bmatrix} \text{ and } \mathbf{K}(L) = \begin{bmatrix} -k_1 - k_r L & k_{-r} & 0 & k_{-1} \\ k_r L & -k_2 - k_{-r} & k_{-2} & 0 \\ 0 & k_2 & -k_{-2} - k_{-d} & k_d L \\ k_1 & 0 & k_{-d} & -k_{-1} - k_d L \end{bmatrix} \tag{2}$$

where $r_a = R_a/R_T$, $c_a = C_a/R_T$, $c_i = C_i/R_T$, $r_i = R_i/R_T$ and k_i's are specific kinematic parameters.
Following the work of Segel et al. [1], we assume that the effect induced by the PTH stimulus is measured by scaled activity α, which is defined as a weighted linear combination of receptors and complexes normalised concentrations as

$$\alpha(L) = a_1 r_a + a_2 c_a + a_3 c_i + a_4 r_i, \tag{3}$$

where a_i's can be viewed as association constants. Subsequently, a scalar value α_R named as cellular responsiveness is computed. To reach the maximum value, the following constrained optimisation problem is solved

[1]Mechanical, Medical and Process Engineering, Queensland University of Technology, Brisbane, QLD 4000, Australia
[2]School of Pharmacy and Medical Sciences, Griffith University, Gold Goast, QLD 4222, Australia
[3]Anatomy, Cell Biology and Physiology, School of Medicine, Indiana University, Indianapolis, United States
[4]Department of Anatomy, Physiology and Pharmacology, University of Saskatchewan, Saskatoon, Canada

$$\max_{(\tau_1,T,\gamma_0,\gamma_1)} \alpha_R(L(\tau_1,T,\gamma_0,\gamma_1,t))) \tag{4}$$

with the constraint that the area under the curve in a (L,t)-plot during an arbitrary time interval does not change. T is the period of one glad burst, γ_0 and γ_1 are the baseline and maximum PTH concentrations, respectively.

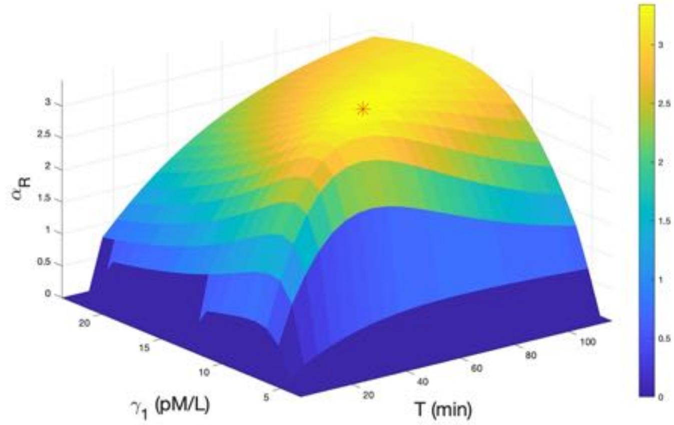

Figure 2: Cellular responsiveness α_R for a healthy person as function of period T and duration and the maximum PTH concentration γ_1. Maximal value is labelled with a red star.

Fig 2 shows the resulting surface plot. The maximal cellular responsiveness is labelled with a red star and its value is $\alpha_R^{max} = 3.35$. The same optimisation procedure can be used to compute an optimal dose of an external PTH drug administration in order to restore a reference value of a_R corresponding to a healthy person [3].

Acknowledgments The work was supported by a fellowship within the IFI programme of the German Academic Exchange Service (DAAD), the Bavarian funding programme BayIntAn and Deutsche Forschungsgemeinschaft (DFG, German Research Foundation) which are gratefully acknowledged.

References

[1] Segel LA, Goldbeter A, Devreotes PN, Knox BE. *A Mechanism for Exact Sensory Adaptation Based on Receptor Modification.* 120(2):151-179, 1986.

[2] Li Y, Goldbeter A. *Frequency Specificity in Intercellular Communication. Influence of Patterns of Periodic Signaling on Target Cell Responsiveness.* Biophysical Journal. 55 (1): 125-145, 1989.

[3] Harms HM, Neubauer O, Kayser C, Wüstermann PR, Horn R, Brosa U et al. *Pulse Amplitude and Frequency Modulation of Parathyroid Hormone in Early Postmenopausal Women before and on Hormone Replacement Therapy.* The Journal of Clinical Endocrinology and Metabolism. 78(1):48-52. 612, 1994.

Different convergence concepts for the Newmark algorithm

Dhananjay Phansalkar, Michael Ortiz[1], Kerstin Weinberg[2], Sigrid Leyendecker

The general focus of this work is the prediction of the crack propagation in brittle material under dynamic loading. Over the years, there are broadly two approaches being developed to understand the fracture in a complex geometry. They are either sharp crack approaches like an extended finite element method (XFEM)[1] or smeared crack approaches like phase-field models [1]. We are interested in the phase-field models for fracture due to their potential to track complex crack paths without any additional ad-hoc algorithms. These phase-field models have an intrinsic length scale parameter ϵ. In our previous work, we developed a variational based approach to compute an optimised spatially varying ϵ along with a corresponding mesh refinement strategy for quasi-static scenarios [2]. We then extended our approach to the case of dynamic phasefield model leading to following action with time $t \in [0, T]$ and the domain Ω

$$\begin{aligned} S(\boldsymbol{u}, \dot{\boldsymbol{u}}, \nabla \boldsymbol{u}, c, \nabla c, \epsilon) &= \int_0^T \int_\Omega \left[\frac{1}{2}\rho \dot{\boldsymbol{u}} \cdot \dot{\boldsymbol{u}} - [1-c]^2 \psi(\boldsymbol{\varepsilon}) - \mathcal{G}_c \left[\frac{c^2+\eta}{2\epsilon} + \frac{\epsilon}{2}|\nabla c|^2 \right] - \beta\epsilon \right] d\boldsymbol{x}\, dt \\ \psi(\boldsymbol{\varepsilon}) &= \frac{1}{2}\boldsymbol{\varepsilon}(\boldsymbol{u}) : [\mathbb{C}\boldsymbol{\varepsilon}(\boldsymbol{u})] = \frac{1}{2}\lambda[\mathrm{tr}(\boldsymbol{\varepsilon})]^2 + \mu[\boldsymbol{\varepsilon} : \boldsymbol{\varepsilon}]. \end{aligned} \tag{1}$$

where $\boldsymbol{u}(\boldsymbol{x}, t)$ is the displacement field, $\dot{\boldsymbol{u}}$ is the temporal derivative of $\boldsymbol{u}$ called velocity, $\boldsymbol{\varepsilon}$ is strain tensor, and $c(\boldsymbol{x})$ is the phase field. Furthermore, $\epsilon(\boldsymbol{x})$ is a spatially varying regularisation parameter, and ρ, $\mathcal{G}_c$, λ and μ are material parameters, while η and β are model and penalty parameters. Minimising the functional (1) yields coupled PDEs. Using the notion of minimum energy, we performed a numerical convergence investigation in a quasi-static system [2]. However, in the dynamic scenario, this is not as straightforward; thus we first analyse a simple ODE problem to investigate different convergence concepts in a numerical framework. Consider a single spring and mass system, as shown in Figure 1, with no additional friction or gravitational acceleration. The behaviour of a general spring-mass system can be modelled by the following action

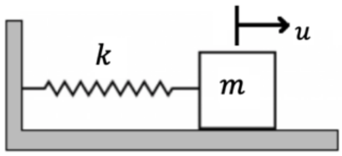

Figure 1: Configuration of spring-mass system

$$S(\boldsymbol{u}, \dot{\boldsymbol{u}}) = \int_0^T L(\boldsymbol{u}, \dot{\boldsymbol{u}}) dt = \int_0^T \left[\frac{1}{2} \dot{\boldsymbol{u}} \cdot \boldsymbol{M} \cdot \dot{\boldsymbol{u}} - \frac{1}{2} \boldsymbol{u} \cdot \boldsymbol{K} \cdot \boldsymbol{u} \right] dt. \tag{2}$$

Here $\boldsymbol{u}(t)$ is the displacement and $\dot{\boldsymbol{u}}$ is the velocity of the mass, while $\boldsymbol{M}$ and $\boldsymbol{K}$ are the mass and stiffness matrices, respectively. The equation of motion for such a spring-mass system is derived by stationarity of the action (2) leading to the following Euler-Lagrange equation.

$$\boldsymbol{M} \cdot \ddot{\boldsymbol{u}} + \boldsymbol{K} \cdot \boldsymbol{u} = \boldsymbol{0} \quad \text{in} \quad (0, T] \tag{3}$$

This second order ODE is discretised using the Newmark method with parameters $\alpha = 0.25$ and $\gamma = 0.5$. The mass and the stiffness used for the simulation of the system depicted in Figure 1 is $m = 0.5$, $k = 1.0$ with initial condition $u(0) = 0.2$, $\dot{u}(0) = v(0) = 0.7$. The simulation is carried out untill $T = 0.1$ with time steps $\Delta t \in \{0.1, 0.01, 0.001, 0.0001\}$. According to the literature [3], with the chosen parameters, the Newmark method has a convergence rate of order 2 for displacements and velocities. This can be validated by comparing the Newmark solution to the analytical result. The analytical solution for such a single spring-mass system is provided by

$$u_\mathrm{a}(t) = u(0)\cos(f \cdot t) + \frac{v(0)}{f}\sin(f \cdot t) \qquad v_\mathrm{a}(t) = -u(0) \cdot f \sin(f \cdot t) + \frac{v(0)}{\cos}(f \cdot t) \tag{4}$$

where $f = \sqrt{k/m}$. The analytical solution (4) are utilised to calculate the error in displacement, velocity, and action given by

$$e_u = \max_{t \in [0,T]} |u(t) - u_\mathrm{a}(t)| \qquad e_v = \max_{t \in [0,T]} |v(t) - v_\mathrm{a}(t)| \qquad e_s = |S - S_\mathrm{a}|. \tag{5}$$

Where S_a is the action computed from the analytical solution. Figure 2, shows the different errors (5) and

[1]Division of Engineering and Applied Sciences, California Institute of Technology, California, USA
[2]Lehrstuhl für Festkörpermechanik, Universität Siegen, 57076 Siegen, Germany

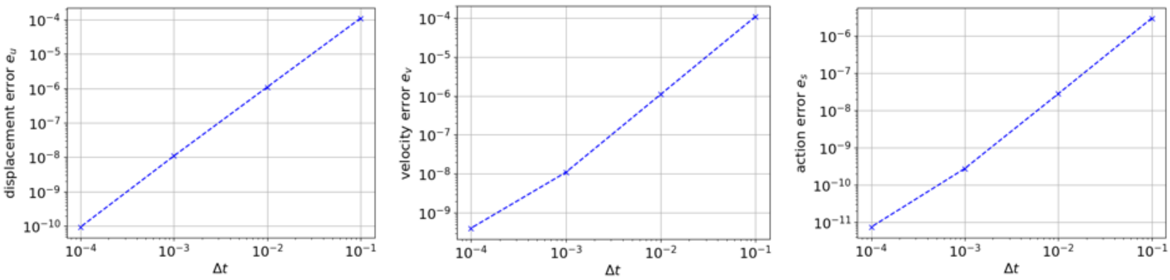

Figure 2: From left to right: Convergence behaviour of displacement, velocity and action

illustrates the convergence behaviour for displacement, velocity, and action. It exhibits quadratic convergence for all three quantities. Because analytical solutions are not always available, we also conduct the convergence analysis based on the approach described in [4]. To accomplish this, we replace the acceleration in equation (3) with Newmark's discrete acceleration, yielding

$$\boldsymbol{M} \cdot \frac{\boldsymbol{u}_{n+1} - \tilde{\boldsymbol{u}}_{n+1}}{\Delta t^2 \alpha} + \boldsymbol{K} \cdot \boldsymbol{u}_{n+1} = \boldsymbol{0} \tag{6}$$

where $\boldsymbol{u}_{n+1}$ is the unknown displacement, and $\tilde{\boldsymbol{u}}_{n+1}$ is the known predictor for the displacement. The solution of the problem (6) is equivalent to a static problem resulting from minimising a potential E with respect to $\boldsymbol{u}_{n+1}$, where E is defined by

$$E(\boldsymbol{u}_{n+1}, \boldsymbol{u}_n, \boldsymbol{v}_n) = \frac{\Delta t^2 \alpha}{2} \frac{\boldsymbol{u}_{n+1} - \tilde{\boldsymbol{u}}_{n+1}}{\Delta t^2 \alpha} \cdot \boldsymbol{M} \cdot \frac{\boldsymbol{u}_{n+1} - \tilde{\boldsymbol{u}}_{n+1}}{\Delta t^2 \alpha} + \frac{1}{2} \boldsymbol{u}_{n+1} \cdot \boldsymbol{K} \cdot \boldsymbol{u}_{n+1} \tag{7}$$

We examine convergence using the potential E in (7) and the action S in (2) . Fitting E and S with a power law reveals quadratic convergence in each variable individually, as depicted in Figures 3 and 4, respectively. The next step is to extend this framework of convergence studies to the phase-field modelling of dynamic fracture.

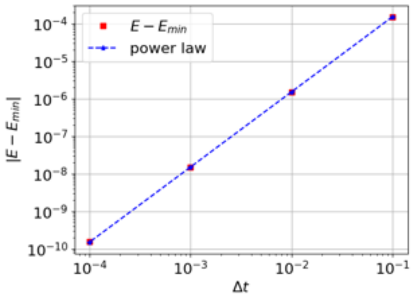

Figure 3: Convergence behaviour of quasi-static potential

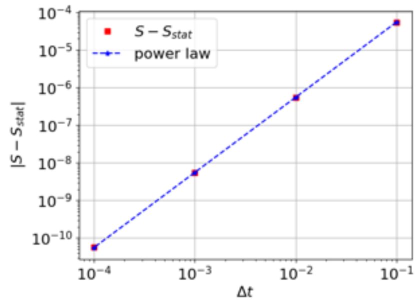

Figure 4: Convergence behaviour of action

Acknowledgement: This research was funded by the Deutsche Forschungsgemeinschaft (DFG, German Research Foundation) - 377472739/GRK 2423/1-2019. The authors are very grateful for this support.

References

[1] A. Egger, U. Pillai, K. Agathos, E. Kakouris, E. Chatzi, I.A. Aschroft and S.P. Triantafyllou.*Discrete and Phase Field Methods for Linear Elastic Fracture Mechanics: A Comparative Study and State-of-the-Art Review.* Applied Sciences, 9:2436, 2019.

[2] D. Phansalkar, K. Weinberg, M. Ortiz and S. Leyendecker. *A Spatially Adaptive Phase-Field Model of Fracture.* Computer Methods in Applied Mechanics and Engineering, 395:114880, 2022.

[3] C. Kane, J.E. Marsden, M. Ortiz and M. West. *Variational Integrators and the Newmark Algorithm for Conservative and Dissipative Mechanical Systems.* International Journal for Numerical Methods in Engineering, 49:1295-1325, 2000.

[4] R. Radovitzky and M. Ortiz. *Error estimation and adaptive meshing in strongly nonlinear dynamic problems.* Computer Methods in Applied Mechanics and Engineering, 172:203-240, 1999.

High order variational integrators for continuum mechanics, constrained mechanical systems and optimal control

Rodrigo T. Sato Martín de Almagro, Sigrid Leyendecker

Geometric integration involves the numerical solution of differential equations using methods that intend to preserve some or all features or underlying structures that the original problem displays.

At our institute, a particular set of geometric integration methods we are interested in is variational methods [1, 2]. These are numerical methods tailored to systems whose behaviour can be derived from a variational principle, e.g. Hamilton's principle of stationary action, and related systems. These systems display important qualitative features that should ideally be present in the results of a simulation, such as conservation laws due to symmetries in the system (Noether's theorem) or compliance with specified constraints.

Variational methods have been widely applied in the numerical simulation of standard mechanical systems such as systems of particles and rigid bodies, as well as optimal control problems, where the dynamics are governed by ordinary differential equations. But these can also be applied to field theories, where the resulting equations are partial differential equations. These include the equations of finite strain elasticity, perfect fluids, electrodynamics, etc. The study and use of variational methods on fields is still not as extended or well-understood as in the former. For that matter, we are trying to understand the basics of these methods.

Currently we are focusing on the following topics:

- **Parallelized variational integrators.** Solving boundary value problems in the context of optimal control of particle systems can be a costly endeavour, particularly for real-time applications. We have analysed the convergence properties of parallelized versions of variational integrators for their implementation in graphics processing units (GPUs) [6]. This has also led us to study very interesting problems in the general theory of discrete Lagrangians. In figure 1, how do you steer a constant-thrust ship to navigate between given points through wind in the minimum time? [5] Different locally optimal solutions of the Zermelo navigation problem solved with a parallel method.

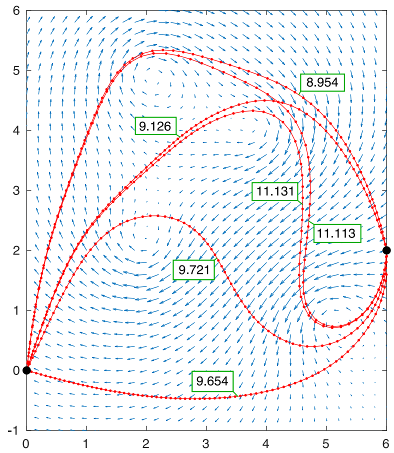

Figure 1: A Zermelo navigation problem.

- **Behaviour of multisymplectic methods.** We are studying multi-symplectic methods [3, 4, 7] in the framework of variational integrators to better understand the properties and expected behaviour of these methods as well as obtain insight into the generation of more general methods. Our main goal is to perform structure-preserving integration of the geometrically exact beam (GEB) (Figure 2).
- **Frequency-dependent dissipation in multisymplectic methods.** We are also interested in the behaviour of multisymplectic methods in the presence of frequency-dependent dissipative terms in the form of external forces and their performance as compared to other methods such as the generalized-α method [8], which displays frequency-dependent numerical dissipation.

References

[1] J. E. Marsden and M. West. Discrete mechanics and variational integrators. *Acta Numerica*, 10:357-514, 2001.

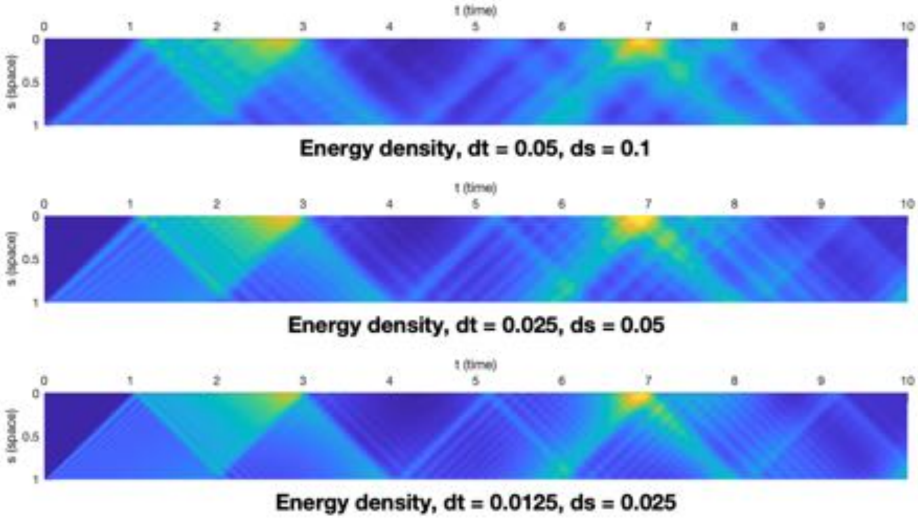

Figure 2: Energy behaviour of the GEB. Evolution in time and space of the energy density of a cantilevered beam under an axial and tangential point loads at the free end. Results on three different grids are displayed.

[2] E. Hairer, C. Lubich, and G. Wanner. Geometric numerical integration: structure preserving algorithms for ordinary diferential equations. *Springer series in computational mathematics.* Springer, Berlin, Heidelberg, New York, 2006.

[3] T. J. Bridges and S. Reich. Multi-symplectic integrators: numerical schemes for Hamiltonian PDEs that conserve symplecticity. *Phys. Lett. A*, 284(4-5):184-193, 2001.

[4] Robert I. McLachlan, Brett N. Ryland, and Yajuan Sun. High order multisymplectic Runge-Kutta methods. *SIAM J. Sci. Comput.*, 36(5):A2199–A2226, 2014.

[5] S. J. Ferraro, D. Martín de Diego and R. T. Sato Martín de Almagro. Parallel iterative methods for variational integration applied to navigation problems. *IFAC-PapersOnLine*, 54(19):321–326, 2021.

[6] S. J. Ferraro, D. Martín de Diego and R. T. Sato Martín de Almagro. A parallel iterative method for variational integration.*(preprint, arXiv:2206.08968).*

[7] T. Leitz, R. T. Sato Martín de Almagro, and S. Leyendecker. Multisymplectic Galerkin Lie group variational integrators for geometrically exact beam dynamics based on unit dual quaternion interpolation. *Comput. Methods Appl. Mech. Eng.*, 374:113475, 2021.

[8] J. Chung and G. M. Hulbert. A time integration algorithm for structural dynamics with improved numerical dissipation: the generalized-α method. *Trans. ASME J. Appl. Mech.*, 60(2):371–375, 1993.

Modelling soft-tissue artefacts with epistemic uncertainty for knee flexion calculations

Eduard S. Scheiterer, Sigrid Leyendecker

A modern method of measuring human movement is optical marker based motion capture. Cameras placed around the moving subject capture the position in space of reflective markers taped to the subjects skin. However, due to the relative motion between skin and the underlying bone, errors are introduced into the measurement, so called soft-tissue artefacts. This error affects any following calculations or evaluations that are based on the marker positions, for instance joint angle calculations. Here, we examine how this error can be modelled and propagated, to give an idea of how much it affects following calculations, in our case, the joint angle.

To do this, the maker data from a measurement of normal human gait is affected with epistemic uncertainty in the form of a triangular fuzzy number. These numbers $\tilde{\boldsymbol{p}}$ define the radius of a sphere for each individual marker around its measured position, as shown in Figure 1. We assume that every marker is within these spheres for the following calculations. The triangular fuzzy number is based on error values from literature and the maximum considered error is modelled for each individual marker, since the error magintude is affected by the markers location on the subjects body. This allows the markers position to vary with an error from their measured position, which enables us to examine the error's effects on following calculations. In order to examine the effects this uncertainty in the markers position has on following calculations, here the joint angle calculation, the uncertainty has to be propagated through the calculations.

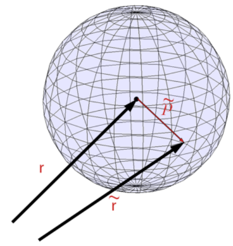

Figure 1: The uncertain marker position $\tilde{\boldsymbol{r}}$ is assumed to be anywhere in a sphere around the measured position $\boldsymbol{r}$.

To propagate the error though the normally deterministic calculations, a special algorithm is required. Epistemic uncertainty that is quantified with fuzzy triangular numbers can be propagated through a calculation with the help of α-level optimisation, see [1]. The results for an exemplary calculation of knee flexion of the left leg during normal human gait over two steps are shown in Figure 2.

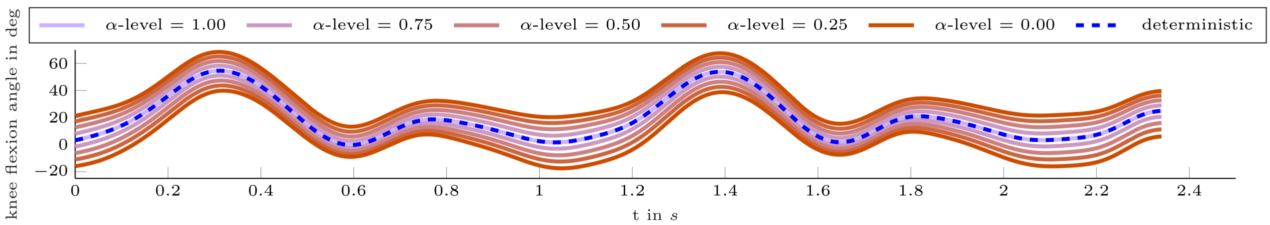

Figure 2: Example of the resulting envelopes of the knee flexion angle of the left leg during normal gate if the marker positions are affected with uncertainty.

As shown, the considered error of up to 32mm for markers leads to considerable deviations in the joint angle. The uncertainty modelling approach and propagation method introduced here can be applied to other movements and joints, that are examined via motion capture. Additionally, it requires only one computation to get the fuzzy output of the joint angles and the resulting error, as opposed to aleatoric (stochastic) simulations, which require many evaluations.

Acknowledgements – This work is partly supported by the German Research Foundation (DFG) as part of the Priority Programme SPP 1886 'Polymorphic uncertainty modelling for the numerical design of structures' (Grant No. LE 1841/4-2).

References

[1] Möller, B. and Beer M.: *Fuzzy randomness: uncertainty in civil engineering and computational mechanics.* Springer Science & Business Media, 2004.

Simulation of spider net dynamics

Matthias Schubert, Sigrid Leyendecker

Spider silk is a fascinating material and subject to active research due to its special properties. Spider silk is very thin and has high specific material properties such as a high Young's Modulus compared to its weight. In collaboration with researchers from Queensland University of Technology (QUT) in Australia, we developed a simulation model for the dynamics of small spider webs, based on a geometrically exact string model. Simulating a spider web accurately entails various challenges. Due to its lightweight, yet exceptional material properties, special attention has to be given to the methods used for the simulation. Otherwise, the spider web may not be represented correctly in the simulation. The geometrically exact string model aims to accurately model the strings strain energy W and calculate the correct behavior throughout the simulation.

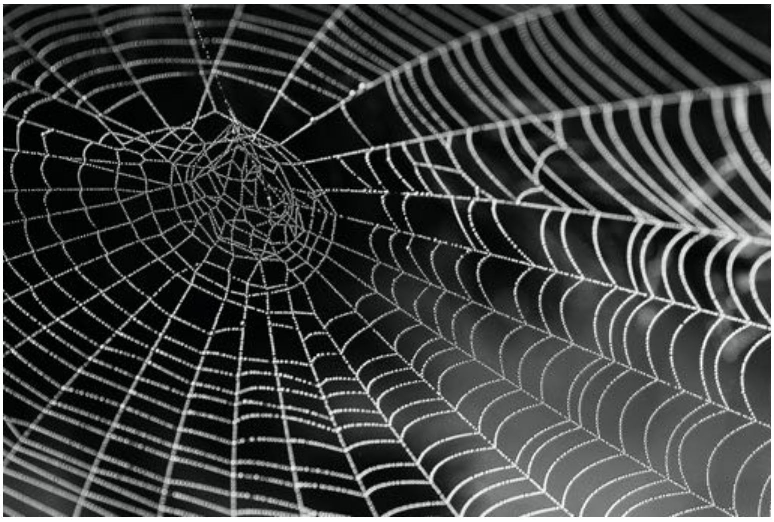

Figure 1: Spider net with connected strings.

To do this, the geometrically exact string model uses a variational integrator in space and time [1]. Such a numerical method preserves momentum and symplectic form. The energy error is bounded. The model features hyper-elastic material models such as Neo-Hook as well as viscous damping to account for material damping. On the one hand, this improves the stability of the numerical simulation. On the other hand, the dissipation of energy in a spider net can be studied with such a model. A version of the code for the simulation of a single string is also published on Github: `https://github.com/THREAD-3-2/GeometricallyExactString`.
The strain energy W for the geometrically exact string has to be adapted compared to the strain energy of a 3D continuum as the geometrically exact string model only includes stretch λ tangential to the center line of the string:

$$W(\lambda) = C_1(\lambda^2 - 1 - 2\ln(\lambda)) + D_1(\lambda - 1)^2. \tag{1}$$

The material parameters C_1 and D_1 are derived via Group Interaction Modelling based on the internal structure of spider silk. There are different types of spider silk that work together in a spider net. Accurate simulation could be a tool to better understand their interaction in the net.

References

[1] Jerrold E. Marsden and Matthew West. Discrete mechanics and variational integrators. *Acta Numerica*, 10:357-514, 2001.

Experimental campaign for mechanical properties characterization of endoscope shafts

Martina Stavole, Vanessa Dörlich, Rodrigo T. Sato Martín de Almagro, Sigrid Leyendecker

Flexible endoscopes are medical devices used for the inspection of internal parts of the body. Their structure is complex, and, in order to study their mechanical behavior, only the outer part, denominated unloaded shaft, is here taken into account. The unloaded shafts are characterized by a hollow slender cylindrical geometry, shown in Fig. 1, and made out of composite materials, i.e. starting from the outer side, two layers of plastic, one layer of stainless steel mesh, and one inner layer of stainless steel coil. Due to the production process and the difficulties of modelling such complex cross-sections, experimental campaigns are fundamental for mechanical parameters characterization. In particular, the results of the testing carried out at ITWM Fraunhofer in Kaiserslautern by using the MeSOMICS machine are here presented.

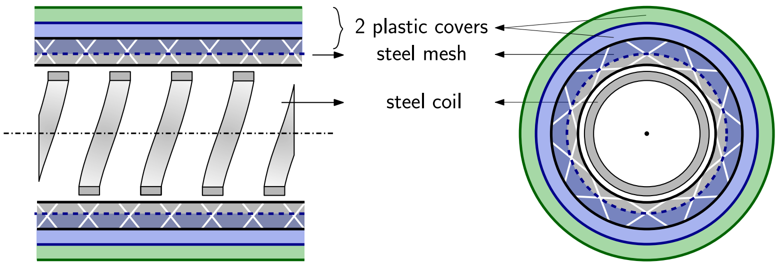

Figure 1: Longitudinal (left) and transversal (right) sections of an unloaded shaft

Tests were run on four endoscope models provided by Karl Storz Estonia, under different conditions and for each model, at least three samples have been tested, firstly under bending and then under torsion. The bending experiments have been performed on the five different types of samples:

- A: samples with long clamping lengths (approximately 30 to 35 cm) without cutting the samples, in order to study the mechanical response under small curvatures.
- B: samples of short clamping lengths as suggested by MeSOMICS without cutting the samples. However, the free length of the endoscopes is too long to run the experiment without physical interference. This is why it was not always performed.
- C: samples that are properly cut according to MeSOMICS's suggestions. A clamping device is used to fix the four layers together from the outside and inside through a cylinder, to avoid the slipping phenomena of the coil while cutting and testing.
- D: samples as described in C, but the coil is removed in order to study its influence on the overall stiffness.
- E: long samples (approximately 30 to 35 cm) without coil after cutting. This test type has been performed only on endoscope 3.

The torsion experiments have been carried out on samples of type C and D. Figure 2 shows the results obtained from the bending experiments on the four shaft models. For each performed test type, the mechanical parameter EI of the samples is shown in the scatter plots in blue. The red dots are the mean values evaluated over this single experiment. One can observe that the values are pretty close to each other, and mostly fall in the 90% confidence intervals (area in green). The same can be noticed for the torsional results shown in Figure 3. Moreover, focusing only on test types C and D (which are the most reliable since they follow the standard MeSOMICS procedure) of the endoscope models 1, 2 and 3, one can see that the average bending and torsional stiffness is in the same range and of the same order, due to the similarities in geometry and structure. Endoscope 4, instead, is characterized by higher stiffness parameters caused by an additional mesh layer.

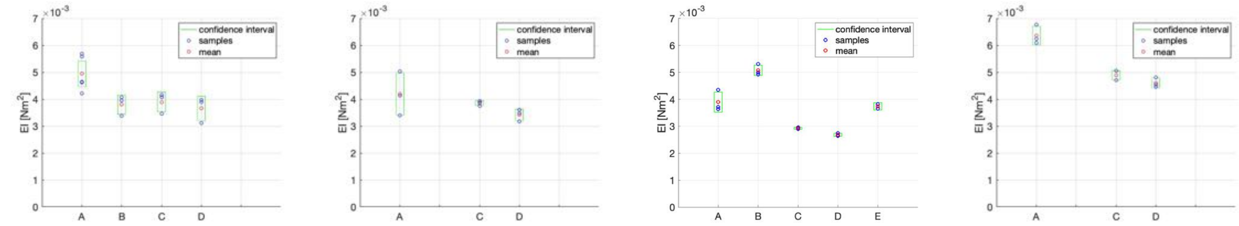

(a) endoscope 1 (b) endoscope 2 (c) endoscope 3 (d) endoscope 4

Figure 2: Bending stiffness of the four endoscope shaft model

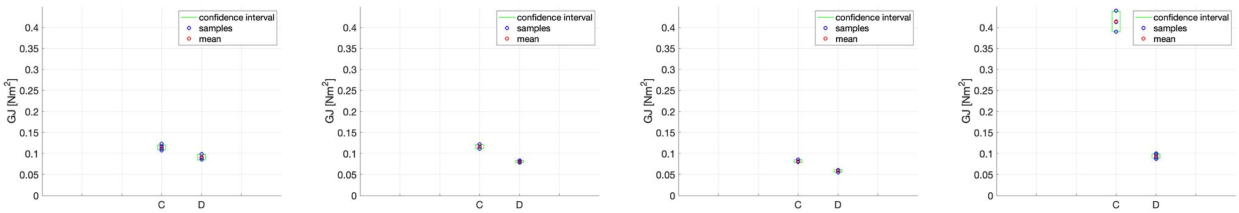

(a) endoscope 1 (b) endoscope 2 (c) endoscope 3 (d) endoscope 4

Figure 3: Torsional stiffness of the four endoscope shaft model

This leads to a deeper study on the contribution of the internal coil on the overall stiffness of the shafts. The following investigation has been made on the short samples by considering test types C and D only. The coil contribution is evaluated as in Equation 1 respectively for bending and torsional stiffness parameters. However, for long samples, the contribution of the coil on the bending stiffness was computed for endoscope 3 only, since only in this case it was possible to carry out test type E and to compare to test type A.

$$\Delta EI_{coil} = \frac{EI_{all\,layers} - EI_{no\,coil}}{EI_{all\,layers}} 100$$
$$\Delta GJ_{coil} = \frac{GJ_{all\,layers} - GJ_{no\,coil}}{GJ_{all\,layers}} 100$$

Results for each endoscope model are shown in terms of percentage in Fig. 4. It can be noticed that the presence of the coil has an influence $\Delta EI_{coil\,short}$ less than 10%. The influence $\Delta GJ_{coil\,short}$ on the torsional stiffness is less than 30% in case of single mesh endoscopes, while it is much higher in case of double mesh endoscopes reaching even 80%.

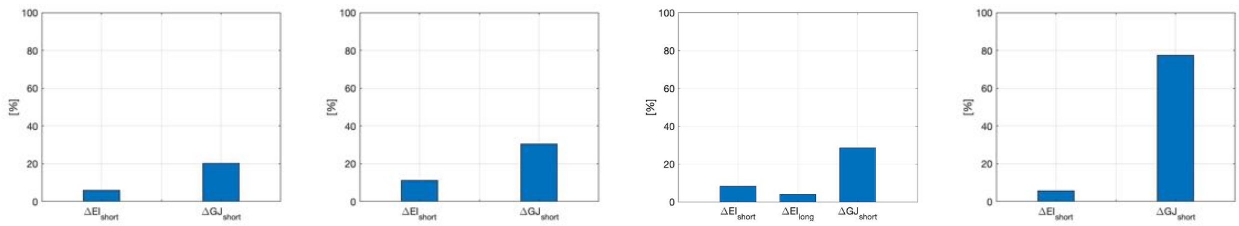

(a) endoscope 1 (b) endoscope 2 (c) endoscope 3 (d) endoscope 4

Figure 4: Influence of the coil on the stiffness parameters of the four endoscope shafts

Acknowledgments This project has received funding from the European Union's Horizon 2020 research and innovation under the Marie Skłodowska-Curie grant agreement No.860124.

4 Activities

4.1 Adjunct professorship QUT

From 01.01.2022 is Prof. Dr.-Ing. habil. Sigrid Leyendecker designated as adjunct Professor at the Faculty of Engineering, School of Mechanical, Medical and Process Engineering at the Queensland University of Technology in Brisbane, Australia, in which Prof. Leyendecker spent several months at campus. Great benefits of academic and cultural exchange were obtained, as well as a solid academic cooperation that will prevail between our institute and QUT, in particular, in the area of biomechanics. Without a doubt, a huge step that broadens the horizons and scope of the research at LTD.

4.2 Research visit to QUT

As part of development of the project, Smoothed finite element methods in modelling and simulation of cardiac electromechanic, M.Sc. Denisa Martonová spent four months at QUT for academic exhange.



4.3 THREAD - Geometric numerical integration, Young Researchers Minisymposium

The minisymposium was organized by M.Sc. Andrea Leone, M.Sc. Ergys Çokaj and M.Sc. Martina Stavole (Marie Curie Fellows at THREAD network) in cooperation with Prof. Dr.-Ing. habil. Sigrid Leyendecker at the Conference on the Numerical Solution of Differential and Differential-Algebraic Equations (NUMDIFF-16).

4.4 Frascal – Mini Lecture: „Introduction to Numerics (INUMS)“

As part of the Frascal qualification programme, LTD offered on 24 June 2022 the Mini Lecture *Introduction to Numerics*, prepared and given by Dr.-Ing. Giuseppe Capobianco, Dr.-Ing. Denpeng Huang, Dr. Rodrigo T. Sato Martín de Almagro and Prof. Dr.-Ing. habil. Sigrid Leyendecker. Lecture notes were created by the team and published for further distribution within the participants.

4.5 Return to lecture halls

During 2022 the Covid-19 pandemic restrictions were progressively withdrawn. All LTD lectures resumed, in both summer and winter semester, presencially in the lecture halls. However, the digital material that was produced during the past years remains available, so more students can benefit from its content.

4.6 Motion capture laboratory

Our motion analysis lab is equipped with a camera and marker based optical tracking system, including 10 Qualisys MoCap high speed cameras and 2 Qualisys high speed video cameras, as well as Noraxon MyoMotion inertial sensors, Cybergloves III to measure hand joint angle kinematics, force plates, and Noraxon Desktop DTS electromyography sensors.

A frame was constructed to bring the cameras closer to the markers in order to perform motion capturing for small human actions, such as motion of hand digits. With this setup, kinematic parameter identification for joints in the human hand, especially the wrist, the metacarpophalangeal and interpalangeal joints has been performed. This is an essential first step towards formulating a procedure for effective parameter identification to setup subject-specific models. This will enable us to perform biomechanical optimal control simulations with higher levels of confidence and use the results as measures of human performance.


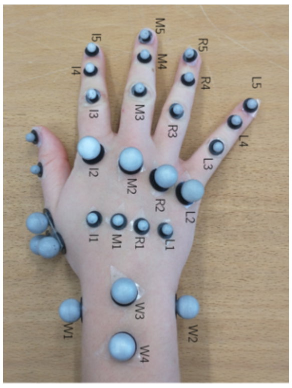
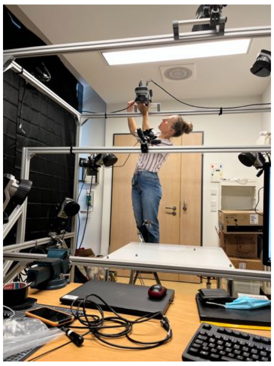
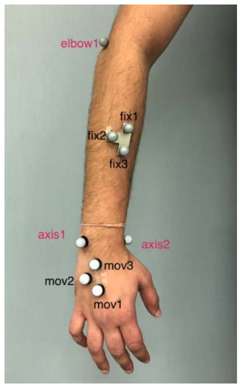

The motion capture laboratory increased its performance by taking a step forward with an extensive measurement program of rheumatoid arthritis and psoriasis arthritis patients, in cooperation with the Department of Medicine 3 - Rheumatology and Immunology of the Universitätsklinikum Erlangen, in the frame of the EmpkinS project. A total of 225 individual measurements were performed for this project in 2022.

- CyberGlove: The analysis of hand movements can yield useful information and indicators for the detection of rheumatic diseases at an early stage. The CyberGlove project goal is to analyze whether the glove bears potential for this purpose. In a second step, we aim to measure activities of daily life and examine if the use of specific joints has an impact on the development of arthritis.

4.7 IT systems

To ensure availability of our server ltd-emmy and to protect against loss of data caused by severe damage or theft of the server hardware, we have installed a backup server in an off-site location. On a nightly schedule, the backup server receives replicas of the ZFS datasets stored on ltd-emmy. To save energy, the backup server, just like any other lab computer at the institute, automatically shuts down after a short idle time and wakes up on demand based on a network request which is issued via the ltd-monitor application. In order to deal with the continuously growing amount of data, the ZFS storage pool of ltd-emmy has been upgraded to its full capacity, namely 24 disks.
To respond to the high demand for workstations which can be used for post-processing of motion-capturing data, we have installed, in addition to ltd-lab11 and ltd-lab18, the two workstations ltd-lab41 and ltd-lab45.
Since we have regularly encountered issues with Apple's Time Machine backup when backing up the staff member's MacBooks, we have now switched to an open-source solution based on SSH and rsync. However, due to security features of macOS which prevent access to Apple's Library folder and also due to some badly behaved applications which cause problems with file permissions for their application data, this alternative backup process unfortunately comes with its own problems. To hopefully have fast and reliable backups for staff laptops in the future, we currently test ZFS on macOS. So far, the experience has been positive. In the

future, this could allow staff members to incrementally send ZFS snapshots to ltd-emmy. Next to speed, the checksum-based storage provided by ZFS would put an end to worrying about completeness of backups.
In contrast to Unix-like operating systems, Windows is by default quite liberal with respect to file permissions. Regular user accounts can write, modify and delete data which is stored directly under drive C, D, etc. To protect against manipulation and theft of data, a Windows Group Policy has been setup in order to restrict access to the owners of such data. At the same time, the previously unprotected data which has accumulated on the workstations over years has mostly been moved to project-specific shares on ltd-emmy. While this policy has been introduced on most lab computers, completion of this project had to be deferred to 2023. Redundancy, snapshots and off-site backup lead to a high price for the storage of ltd-emmy. In order to reserve capacity for future years, it has been decided to offload important, but in principle reproducible artifacts to a cheaper storage medium which shall be installed in the new year.

4.8 Editorial activities

Advisory and editorial board memberships Since January 2014, Prof. Dr.-Ing. habil. Sigrid Leyendecker is a member of the advisory board of the scientific journal Multibody System Dynamics, Springer. She is a member of the Editorial Board of ZAMM – Journal of Applied Mathematics and Mechanics / Zeitschrift für Angewandte Mathematik und Mechanik since January 2016 and since 2017 runs a second term as member of the managing board of the International Association of Applied Mathematics and Mechanics (GAMM), as well as a member of the executive council of the German Association for Computational Mechanics (GACM) and member of the General Council of the International Association for Computational Mechanics (IACM).

Since October 2017, Prof. Dr.-Ing. habil. Sigrid Leyendecker is an elected member of the Faculty Council of the Faculty of Engineering at the Friedrich-Alexander-Universität Erlangen-Nürnberg, and in April 2019 was elected deputy Chair of the Qualification Assessment Committee (Eignungsfeststellungsverfahrens -(EFV-)Kommission) of the Bachelor's degree programme Medical Engineering, at the Friedrich-Alexander-Universität Erlangen-Nürnberg.

5 Teaching

Winter semester 2022/2023

Dynamik starrer Körper (MB, ME, WING, IP, BPT, CE, MT)		
Vorlesung		S. Leyendecker
Übung + Tutorium		G. Capobianco, X. Chen D. Huang, D. Holz, M. Schubert
Mehrkörperdynamik (MB, ME, WING, TM, BPT, MT)		
Vorlesung		S. Leyendecker
Übung		M. Schubert R.T. Sato Martín de Almagro
Praktikum Technische Dynamik – Modellierung, Simulation und Experiment (MB, ME, WING)		
		S. Leyendecker X. Chen, D. Holz, D. Phansalkar R.T. Sato Martín de Almagro
Praktikum Matlab (MB)		
		S. Leyendecker D. Phansalkar, M. Stavole

Summer semester 2022

Biomechanik (MT)		
Vorlesung + Übung		G. Capobianco
geprüft	36 + 19 (WS 2021/2022)	
Geometric numerical integration (MB, ME, WING, BPT)		
Vorlesung		S. Leyendecker R.T. Sato Martín de Almagro
Übung		R.T. Sato Martín de Almagro
geprüft	3 + 0 (WS 2021/2022)	
Statik und Festigkeitslehre (BPT, CE, ME, MWT, MT)		
Vorlesung		S. Leyendecker, G. Capobianco
Tutorium		X. Chen, D. Holz, D. Huang, M. Schubert
Übung		X. Chen, D. Holz, M. Schubert
geprüft	324 + 179 (WS 2021/2022)	
Praktikum Matlab (MB)		
Teilnehmer	47	S. Leyendecker D. Huang

Winter semester 2021/2022

Dynamik starrer Körper (MB, ME, WING, IP, BPT, CE, MT)		
Vorlesung		S. Leyendecker
Tutorium		G. Capobianco, D. Holz D. Martonová, T. Wenger
Übung		D. Holz, D. Martonová M. Schubert
geprüft	253 + 110 (SS 2022)	
Mehrkörperdynamik (MB, ME, WING, TM, BPT, MT)		
Vorlesung		S. Leyendecker
Übung		T. Wenger
geprüft	71 + 30 (SS 2022)	
Geometric beam theory (MB, ME, WING, BPT)		
Vorlesung + Übung		S. Leyendecker R.T. Sato Martín de Almagro
Praktikum Technische Dynamik – Modellierung, Simulation und Experiment (MB, ME, WING)		
Teilnehmer	10	S. Leyendecker G. Capobianco, D. Holz R.T. Sato Martín de Almagro M. Schubert
Praktikum Matlab (MB)		
Teilnehmer	66	S. Leyendecker M. Schubert

5.1 Theses

Doctoral theses

- Dr.-Ing. Thomas Leitz
  Galerkin Lie group variational integrators
- Dr.-Ing. Johann Penner
  A discrete variational approach to muscle wrapping in musculoskeletal optimal control simulations

Master theses

- Julian Lang
  Estimation of index finger joint loads from daily activities experiments

Project theses

- Julian Hübner
  Estimating spinal curvature and spinal mobility based on inertial measurement unit data

Bachelor theses

- Isabella Reiher
  On the advanced calibration of CyberGlove III and its applicability for rheumatic patients
- Johannes Michaelis
  Development of a Python-based communication interface for CyberGlove III and comparison of calibration methods

5.2 Seminar for mechanics

together with the Chair of Applied Mechanics LTM

21.12.2022 M.Sc. Flóra Orsolya Szemenyei
Department Mathemaik
Friedrich-Alexander-Universtität Erlangen-Nürnberg
Besov regularity of parabolic PDEs with inhomogeneous boundary conditions

19.12.2022 M.Sc. Rohan Deo
Leibniz Universität Hannover
Multiphase flow poromechanical modeling of living tissue

29.11.2022 Dr.-Ing. Silvia Budday
Friedrich-Alexander-Universtität Erlangen-Nürnberg
Prof. Stéphane Bordas, Dr. Stéphane Urcun and Dr. Anas Obeidat
University of Luxembourg
Multiphase flow poromechanical modeling of living tissue

25.05.2022 M.Sc. Indrajeet Patil
University of Liège, Belgium
A nonsmooth geometric approach for system-level modelling of braiding process

30.03.2022 Prof. Francesco dell'Isola
DICEAA and Memocs
Università dell'Aquila
The materialisation of the Eudoxus' model for the motion of planets and the similar materialisation of the abstract concept of forceand internal tension

19.01.2022	Prof. Alessandro Del Vecchio Department Artificial Intelligence in Biomedical Engineering Friedrich-Alexander-Universtität Erlangen-Nürnberg *Deep learning human movement: an example of the neuromuscular control of the human hand*

5.3 Computational Multibody Dynamics

A new course called "Computational Multibody Dynamics" has been devised and taught by Dr.-Ing. Giuseppe Capobianco. During this course, the students learn to understand and implement a modular software for the simulation of multibody systems. After a concise treatment of the theory of multibody dynamics, the translation of the theory into a simulation software is discussed. This is complemented with several programming exercises enabling the students to gain practical experience and a profound understanding of the modular software structure. By taking this course, the students will be able to

- write their own code for the simulation of complex multibody systems.
- understand what goes on "under the hood" of commercial multibody simulation software.

5.4 Dynamic laboratory

The dynamic laboratory – modeling, simulation and experiment (Praktikum Technische Dynamik) adresses all students of the Technical Faculty of the Friedrich-Alexander-Universität Erlangen-Nürnberg. The aim of the practical course is to develop mathematical models of fundamental dynamical systems to simulate them numerically and compare the results to measurements from the real mechanical system. Here, the students learn both the enormous possibilities of computer based modeling and its limitations. The course contains one central programming exercise and six experiments observing various physical phenomena along with corresponding numerical simulations:

- programming exercise
- beating pendulums
- gyroscope
- ball balancer system
- robot arm
- inverse pendulum
- balancing robot

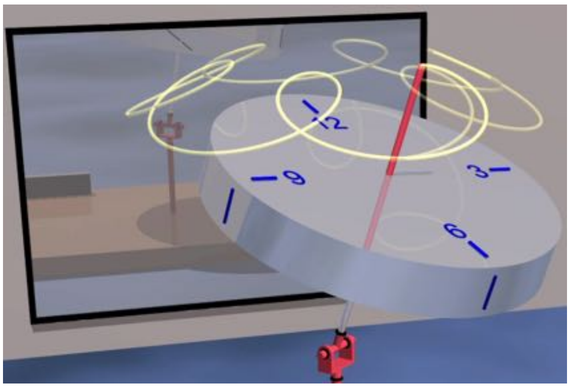

programming exercise

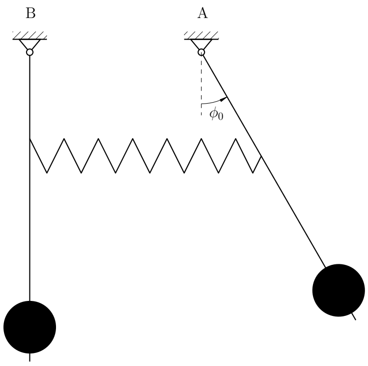

beating pendulums

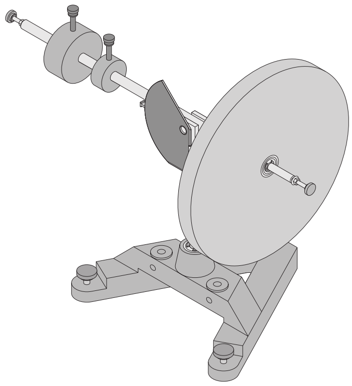

gyroscope

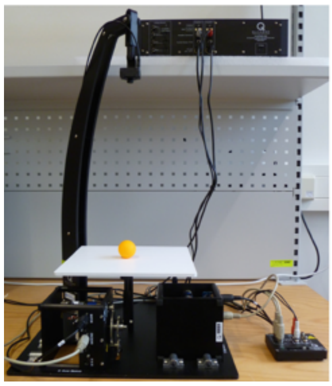

ball balancer system

robot arm

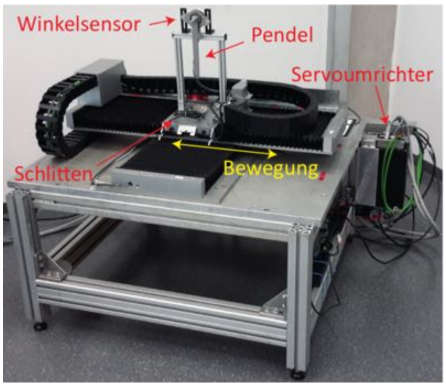

inverse pendulum

balancing robot

5.5 MATLAB laboratory

The MATLAB laboratory (Praktikum MATLAB) is offered to all students of the Technical Faculty of the Friedrich-Alexander-Universität Erlangen-Nürnberg. The course aims to teach the participants the basic skills of numerical programming in MATLAB. The course is offered in conjunction with the Institute of Applied Mechanics (LTM), the Institute of Production Metrology (FMT) and the Institute of Engineering Design (KTmfk). The first lecture is an introductory programming session for MATLAB fundamentals. Thereafter, every institute presents a task related to mechanics and engineering, for example, the LTD task is to understand and simulate, the dynamics of a crane. The task is introduced to the students through a theory lecture, which is then followed by programming sessions.

6 Publications

6.1 Reviewed journal publications

1. J. Penner and S. Leyendecker. "A discrete mechanics approach for musculoskeletal simulations with muscle wrapping". *Multibody System Dynamics*, pp. 1-21, DOI 10.1007/s11044-022-09844-x, 2022.
2. E.S. Scheiterer and S. Leyendecker. "Fuzzy forward dynamics of distinct gait phases with a prosthetic foot". *Computational Mechanics*, Vol. 70 pp. 501-513 DOI 10.1007/s00466-022-02167-w, 2022.
3. D. Phansalkar, K. Weinberg, M. Ortiz and S. Leyendecker. " A spatially adaptive phase-field model of fracture". *Computer Methods in Applied Mechanics and Engineering*, Vol. 395 DOI 10.1016/j.cma.2022.114880, 2022.
4. D. Huang and S. Leyendecker. "Optimal control of dielectric elastomer actuated multibody dynamical systems". *arXiv – Computational Engineering, Finance, and Science*, arXiv:2207.06424, DOI 10.48550/arXiv.2207.06424, 2022.
5. X. Chen, S. Leyendecker and H. van den Bedem. "Kinematic Vibrational Entropy Assessment and Analysis of SARS CoV-2 Main Protease". *Journal of Chemical Information and Modeling*, Vol. 62(11) pp. 2869-2879, DOI 110.1021/acs.jcim.2c00126, 2022.
6. D. Martonová, D. Holz, D. Brackenhammer, M. Weyand, M. Alkassar and S. Leyendecker. "Support Pressure Acting on the Epicardial Surface of a Rat Left Ventricle – A Computational Study". *Frontiers in Cardiovascular Medicine*, Vol. 9, DOI 10.3389/fcvm.2022.850274, 2022.
7. D. Martonová, D. Holz, J. Seufert, M.T. Duong, M. Alkassar and S. Leyendecker. "Comparison of stress and stress–strain approaches for the active contraction in a rat cardiac cycle model". *Journal of Biomechanics*, Vol. 134, pp. 110980, DOI doi.org/10.1016/j.jbiomech.2022.110980, 2022.
8. U. Phutane, M. Roller and S. Leyendecker. "Optimal control simulations of two finger grasps". *Mechanism and Machine Theory*, Vol. 167, pp. 104508, DOI doi.org/10.1016/j.mechmachtheory.2021.104508, 2022.

6.2 Invited lectures

1. G. Capobianco, D. Huang, R.T. Sato Martín de Almagro and S. Leyendecker. "Introduction to Numerics (INUMS)". *FRASCAL Mini Lecture*, Erlangen, Germany, 24 June, 2022

6.3 Conferences and proceedings

1. M. Stavole, R.T. Sato Martín de Almagro, M. Lohk and S. Leyendecker. "Homogenization of the constitutive properties of composite beam cross-sections', *Computational Solid Mechanics*, DOI 10.23967/eccomas.2022.139, 2022.
2. M. Nitschke, R. Marzilger, S. Leyendecker, B. Eskofier, A. Koelewijn. "Change the direction: 3D optimal control simulation by directly tracking marker and ground reaction force data", *bioRxiv*, DOI 10.1101/2022.08.02.502455, 2022.
3. D. Huang and S. Leyendecker. "Optimal control of dielectric elastomer actuated multibody dynamical systems', *arXiv preprint arXiv:2207.06424*, 2022.
4. M. Lohmayer and S. Leyendecker. "EPHS: A Port-Hamiltonian Modelling Language", *arXiv preprint arXiv:2202.00377*, 2022.
5. M. Lohmayer and S. Leyendecker. "Exergetic Port-Hamiltonian Systems: Navier-Stokes-Fourier Fluid", IN: *Proceedings of the IFAC Workshop on Thermodynamics Foundations of Mathematical Systems Theory TFMS*, Montreal, Canada, Vol. 55(18), pp. 74-80, DOI /10.1016/j.ifacol.2022.08.033, 2022.
6. M. Stavole and S. Leyendecker. "Industrial and mathematical challenges of a medical application". *FAU Schnupper-Uni 2022*, Erlangen, Germany 4 November, 2022.
7. S. Heinrich, U. Phutane, B. Coppers, A. M. Liphardt and S. Leyendecker. "Towards optimal control grasping simulations with the full hand". *9th GACM Colloquium on Computational Mechanics - for Young Scientists from Academia and Industry*, Essen, Germany 21-23 September, 2022.

8. M. Lohmayer and S. Leyendecker. “EPHS: A Port-Hamiltonian Modelling Language’. *MTNS 2022: 25th International Symposium on Mathematical Theory of Networks and Systems*, Bayreuth, Germany 12-16 September, 2022.
9. P. Kumar, D. Phansalkar, J. Mergheim, S. Leyendecker and P. Steinmann. “Computational Fracture Modeling in Heterogeneous Materials - Recent Advances and Future Challenges”. *CCM-APCOM 15th World Congress on Computational Mechanics & 8th Asian Pacific Congress on Computational Mechanics*, Yokohama, Japan (online) 31 July - 5 August, 2022.
10. E.S. Scheiterer and S. Leyendecker. “Considering epistemic uncertainty in optical marker based joint angle calculation during human gait”. *CCM-APCOM 15th World Congress on Computational Mechanics & 8th Asian Pacific Congress on Computational Mechanics*, Yokohama, Japan (Online), 31 July - 5 August, 2022.
11. M. Lohmayer and S. Leyendecker. “Exergetic Port-Hamiltonian Systems: Navier-Stokes-Fourier Fluid”. *TFMST 2022: IFAC Workshop on Thermodynamic Foundations of Mathematical Systems Theory*, Montreal, Canada (Online), 24-27 July, 2022.
12. M. Stavole, V. Dörlich, J. Linn, R.T. Sato Martín de Almagro and S. Leyendecker.“Endoscopes: an experimental characterisation of their constitutive properties”. *ITWM Fraunhofer*, Kaiserslautern, Germany, 22 July, 2022.
13. S. Heinrich, U. Phutane, J. Penner, B. Coppers, A.M. Liphardt and S. Leyendecker. “Comparison of different approaches for the personalization of a kinematic hand model”. *World Biomechanics Congress 2022*, Taipei, Taiwan (Online), 10-14 July, 2022.
14. B. Coppers, U. Phutane, D. Berisha, K. Tascilar, A. Kleyer, D. Simon, J. Bräunig, J. Penner, M. Vossiek, V. Schönau, S. Heinrich, S. Bayat, G. Schett, S. Leyendecker and A.M. Liphardt. “Establishment and evaluation of a sensor-based method to assess hand function in patients with rheumatoid arthritis”. *World Biomechanics Congress 2022*, Taipei, Taiwan (Online), 10-14 July, 2022.
15. B. Coppers, S. Heinrich, U. Phutane, D. Berisha, K. Tascilar, A. Kleyer, D. Simon, J. Bräunig, J. Penner, M. Vossiek, V. Schönau, S. Bayat, G. Schett, S. Leyendecker and A.M. Liphardt. “Evaluation of marker-based motion capturing to charactherize basic hand movements in rheumatic patients”. *27th Congress of the European Society of Biomechanics*, poster, Porto, Portugal, 26-29 June, 2022.
16. D. Holz, D. Martonová, E. Schaller, M.T. Duong, M. Alkassar and S. Leyendecker. “The influence of the orthotropic tissue in an electromechanical heart model”. *27th Congress of the European Society of Biomechanics*, Porto, Portugal, 26-29 June, 2022.
17. D. Phansalkar, K. Weinberg, M. Ortiz and S. Leyendecker. “A spatially adaptive phase-field model for dynamic fracture”. *ECCOMAS - 8th European Congress on Computational Methods in Applied Sciences and Engineering*, Oslo, Norway, 5-9 June, 2022.
18. M. Stavole, R.T. Sato Martín de Almagro, M. Lohk and S. Leyendecker. “Homogenization of the constitutive properties of composite beam cross-sections”. *ECCOMAS - 8th European Congress on Computational Methods in Applied Sciences and Engineering*, Oslo, Norway, 5-9 June, 2022.
19. M. Stavole and S. Leyendecker. “Industrial and mathematical challenges of a medical application”. *Math meets industry*, Trondheim, Norway, 2 June, 2022.
20. B. Coppers, S. Heinrich, U. Phutane, D. Berisha, K. Tascilar, A. Kleyer, D. Simon, J. Bräunig, J. Penner, M. Vossiek, V. Schönau, S. Bayat, G. Schett, S. Leyendecker and A.M. Liphardt. “Feasibility of using optoelectronic measurement of hand movement for characterizing hand function in rheumatoid arthritis”. *75th EULAR (European Alliance of Associations for Rheumatology) European Congress of Rheumatology 2022*, poster, Copenhagen, Denmark 1-4 June, 2022.
21. M. Stavole and S. Leyendecker. “Variational modelling and simulation of complex beams and their optimisation”. *THREAD Annual Meeting*, Seville, Spain, 26 May, 2022.
22. D. B. Jadhav and S. Leyendecker. “Finite Element Modeling of Osteoporotic Pelvic Ring and Extension of Project P9 into temporal adaptivity”. *2nd RTG Retreat of FRASCAL*, Bad Windsheim, Germany 5-6 May, 2022.

23. M. Stavole, S. Leyendecker and R.T. Sato Martín de Almagro. “Homogenization of the constitutive properties of composite beam cross-sections”. *MaGIC 2022: Manifolds and Geometric Integration Colloquia*, Ilsetra, Norway, 28 February - 4 March, 2022.
24. S. Heinrich and S. Leyendecker. “Analysis of Degenerative Motion Impairments through Integration of Empathokinaesthetic Sensor Data in Biomechanical Human Models”. *EmpkinS GAP IX Workshop*, Erlangen, Germany 1 February, 2022.

7 Social events

Onboarding lunch of team members

Summer fest of the Faculty of Engineerig

Student summer grill



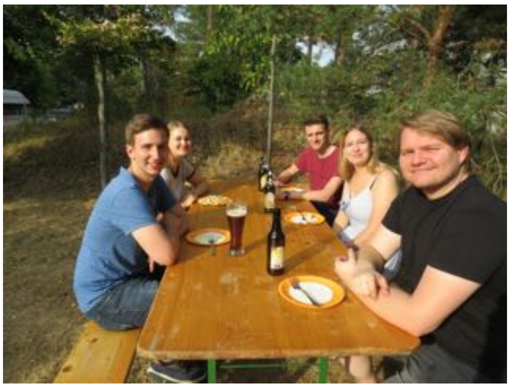



Kayak tour

Doctoral defenses

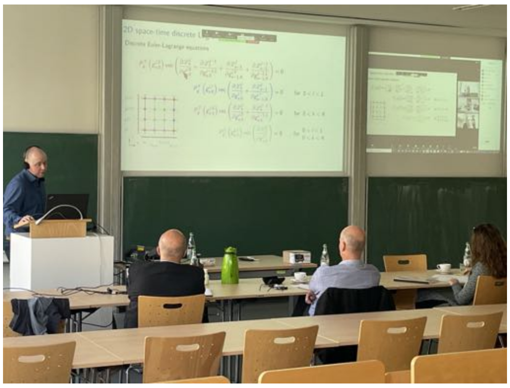

Nikolaus hiking


Farewell of team members